pharmaceuticals

MDPI

Article

Bioactive Compounds from *Euphorbia usambarica* Pax. with HIV-1 Latency Reversal Activity

Yu-Chi Tsai [1], Racheal A. Nell [2], Jonathan E. Buckendorf [2], Norbert Kúsz [1], Peter Waweru Mwangi [3], Róbert Berkecz [4], Dóra Rédei [1], Andrea Vasas [1], Adam M. Spivak [2,*] and Judit Hohmann [1,5,*]

1 Interdisciplinary Excellence Centre, Department of Pharmacognosy, University of Szeged, H-6720 Szeged, Hungary; yuchi0713@gmail.com (Y.-C.T.); kusznorbert@gmail.com (N.K.); redei@pharmacognosy.hu (D.R.); vasasa@pharmacognosy.hu (A.V.)
2 Department of Medicine, University of Utah School of Medicine, Salt Lake City, UT 84132, USA; racheal.nell@outlook.com (R.A.N.); jonny.buckendorf@path.utah.edu (J.E.B.)
3 Department of Medical Physiology, School of Medicine, University of Nairobi, Nairobi P.O. Box 30197-00100, Kenya; waweruk2001@gmail.com
4 Department of Medical Chemistry, University of Szeged, H-6720 Szeged, Hungary; berkecz.robert@szte.hu
5 Interdisciplinary Centre of Natural Products, University of Szeged, H-6720 Szeged, Hungary
* Correspondence: adam.spivak@hsc.utah.edu (A.M.S.); hohmann.judit@szte.hu (J.H.)

Abstract: *Euphorbia usambarica* is a traditional medicine used for gynecologic, endocrine, and urogenital illnesses in East Africa; however, its constituents and bioactivities have not been investigated. A variety of compounds isolated from *Euphorbia* species have been shown to have activity against latent HIV-1, the major source of HIV-1 persistence despite antiretroviral therapy. We performed bioactivity-guided isolation to identify 15 new diterpenoids (**1**–**9**, **14**–**17**, **19**, and **20**) along with 16 known compounds from *E. usambarica* with HIV-1 latency reversal activity. Euphordraculoate C (**1**) exhibits a rare 6/6/3-fused ring system with a 2-methyl-2-cyclopentenone moiety. Usambariphanes A (**2**) and B (**3**) display an unusual lactone ring constructed between C-17 and C-2 in the jatrophane structure. 4β-Crotignoid K (**14**) revealed a 250-fold improvement in latency reversal activity compared to crotignoid K (**13**), identifying that configuration at the C-4 of tigliane diterpenoids is critical to HIV-1 latency reversal activity. The primary mechanism of the active diterpenoids **12**–**14** and **21** for the HIV-1 latency reversal activity was activation of PKC, while lignans **26** and **27** that did not increase CD69 expression, suggesting a non-PKC mechanism. Accordingly, natural constituents from *E. usambarica* have the potential to contribute to the development of HIV-1 eradication strategies.

Keywords: *Euphorbia usambarica*; diterpenoid; usambariphane; HIV; latency reactivation; latency reversal agent; PKC

Citation: Tsai, Y.-C.; Nell, R.A.; Buckendorf, J.E.; Kúsz, N.; Mwangi, P.W.; Berkecz, R.; Rédei, D.; Vasas, A.; Spivak, A.M.; Hohmann, J. Bioactive Compounds from *Euphorbia usambarica* Pax. with HIV-1 Latency Reversal Activity. *Pharmaceuticals* **2021**, *14*, 653. https://doi.org/10.3390/ph14070653

Academic Editor: Daniela De Vita

Received: 3 June 2021
Accepted: 30 June 2021
Published: 7 July 2021

1. Introduction

Antiretroviral therapy (ART) durably blocks HIV-1 transcription by targeting viral enzymes; however, these drugs do not result in viral eradication due to the presence of replication-competent proviruses that are stably integrated into the genomes of a small population of long-lived memory T cells, known as the latent reservoir [1]. A promising strategy to address HIV-1 persistence is to use small molecules to reactivate latent proviruses in order to expose these cells to immune clearance and/or viral cytopathic effect. Natural products offer much promise regarding the discovery of new latency reversal agents (LRAs) for HIV-1 eradication [2–4].

The *Euphorbia* is one of the largest genera in Euphorbiaceae [5,6]. There are many bioactive secondary metabolites in the genus *Euphorbia*, including more than 20 different types of diterpenoids (abietane, atisane, casbane, daphnane, ingenane, jatrophane, karane, lathyrane, tigliane, and others) [7]. Moreover, sesquiterpenoids, triterpenoids, flavonoids, alkaloids, polyphenols, tannins, volatile compounds, and phytosterols have

also been discovered in *Euphorbia* species, many of which are in active use as traditional medicines [8–10]. The pharmacological effects of *Euphorbia* species are related to anti-inflammatory [11], multidrug-resistance-reversing [12,13], antiviral [14,15], cytotoxic [16,17], anti-arrhythmic [18], antifungal [19], anti-thrombotic [20], antiallergic [21], and muscle relaxant [22] properties.

In past, several *Euphorbia* plants have previously been evaluated to determine their efficacy as LRAs [23–30]. For instance, Liu et al. reported the effects on HIV-1 transcription of ingenane esters 3-angeloylingenol and 3-(2-naphthoyl)ingenol from *E. kansui*, which can reactivate latent HIV with EC_{50} values at 4.2 and 2.4 nM, respectively [28]. Yan et al. published atisane diterpenoids euphorneroid D and *ent*-3-oxoatisan-16*α*,17-acetonide from *E. neriifolia* which showed anti-HIV-1 activities with EC_{50} values at 34 and 24 μM, respectively [29]. Valadão et al. established deoxyphorbol esters from *E. umbellata* which increased HIV-1 latency reactivation through NF-κB activation, nuclear translocation, and HIV-1 LTR promoter [30].

Euphorbia usambarica Pax. distributes mainly in East Africa [31] and is a large branching shrub as well as used as a traditional medicine for gynecologic, endocrine, and urogenital illnesses [32,33]. In our preliminary study, we found that the whole plant extract of *E. usambarica* showed a significant HIV-1 latency reversal activity. However, there was no study related to the chemical constituents and bioactivities of *E. usambarica* in the reported literature. In addition, the prevention and treatment of HIV infection and acquired immune deficiency syndrome (AIDS) are still the central issues around the world. Therefore, we would investigate the active constituents and the pharmacological effect of *E. usambarica*. Further, we sought to test its aqueous, and organic fractions for HIV-1 latency reversal activity and cytotoxicity. Dichloromethane and *n*-hexane fractions showed increased activity compared to the whole plant extract (EU) in dose-response analysis. Further sub-fractionation of the active fractions was followed by compounds purification and identification using multistep chromatography, NMR, and mass spectroscopy to yield 31 purified compounds. Six of those compounds demonstrated HIV-1 anti-latency activity. Extended dose-response curves were then generated for these compounds. Several of these compounds have no previously described anti-HIV-1 or anti-latency activity. These results support further exploration of medicinal plants, and *Euphorbia* species in particular, as sources of new means to address HIV-1 persistence.

2. Results

2.1. Structure Elucidation of New Compounds

The partitioned *n*-hexane (EU-H) and dichloromethane (EU-C) phases significantly improved upon reactivation efficacy compared to the EU. The EU-H reactivated latent HIV-1 to 91% at concentrations of 50 and 100 μg/mL. The EU-C phase reactivated latent HIV-1 up to 86% at 10 μg/mL concentration and 98% at 50 μg/mL. The partitioned ethyl acetate (EU-E) and water-soluble residue (EU-W) phases did not appear to have any activity (Figure 1A). Cell viability declined steeply above concentrations of 100 μg/mL. Significant toxicity at concentrations above 100 μg/mL limits conclusions about reactivation. The lower concentrations of the EU-H and EU-C fractions did not affect toxicity but markedly improved viral reactivation (Figure 1B). Due to the high reactivation ratio (86%) at the lowest tested concentration (10 μg/mL), the EU-C phase was selected for bioactivity-guided isolation. This led to identification of 15 new diterpenoids (**1**–**9**, **14**–**17**, **19**, and **20**) along with 16 known compounds (**10**–**13**, **18**, and **21**–**31**) (Figure 2).

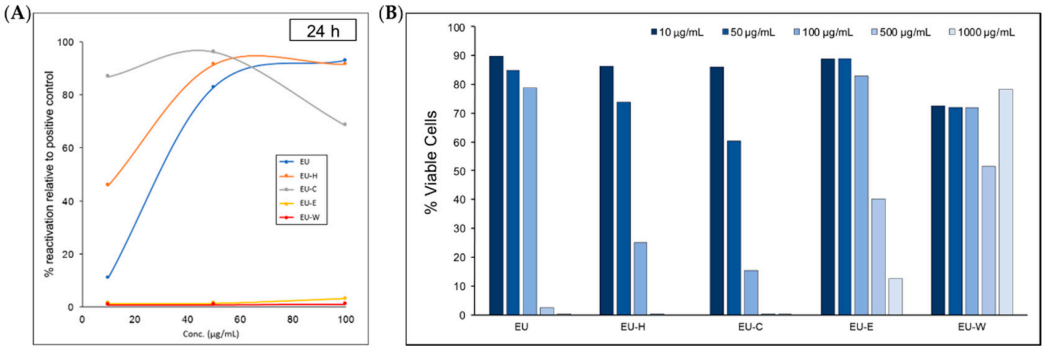

Figure 1. HIV-1 latency reversal activity of methanolic crude extract (EU), partitioned *n*-hexane (EU-H), dichloromethane (EU-C), ethyl acetate (EU-E), and water-soluble residue (EU-W) phases. (**A**) dose-response experiments conducted with Jurkat T cells that were latently infected with full-length HIV-1 reporter construct (J-Lat 10.6 cells), HIV-1 reactivation quantified as % of positive control (PMA); (**B**) cell viability of each sample at 10, 50, 100, 500, and 1000 µg/mL.

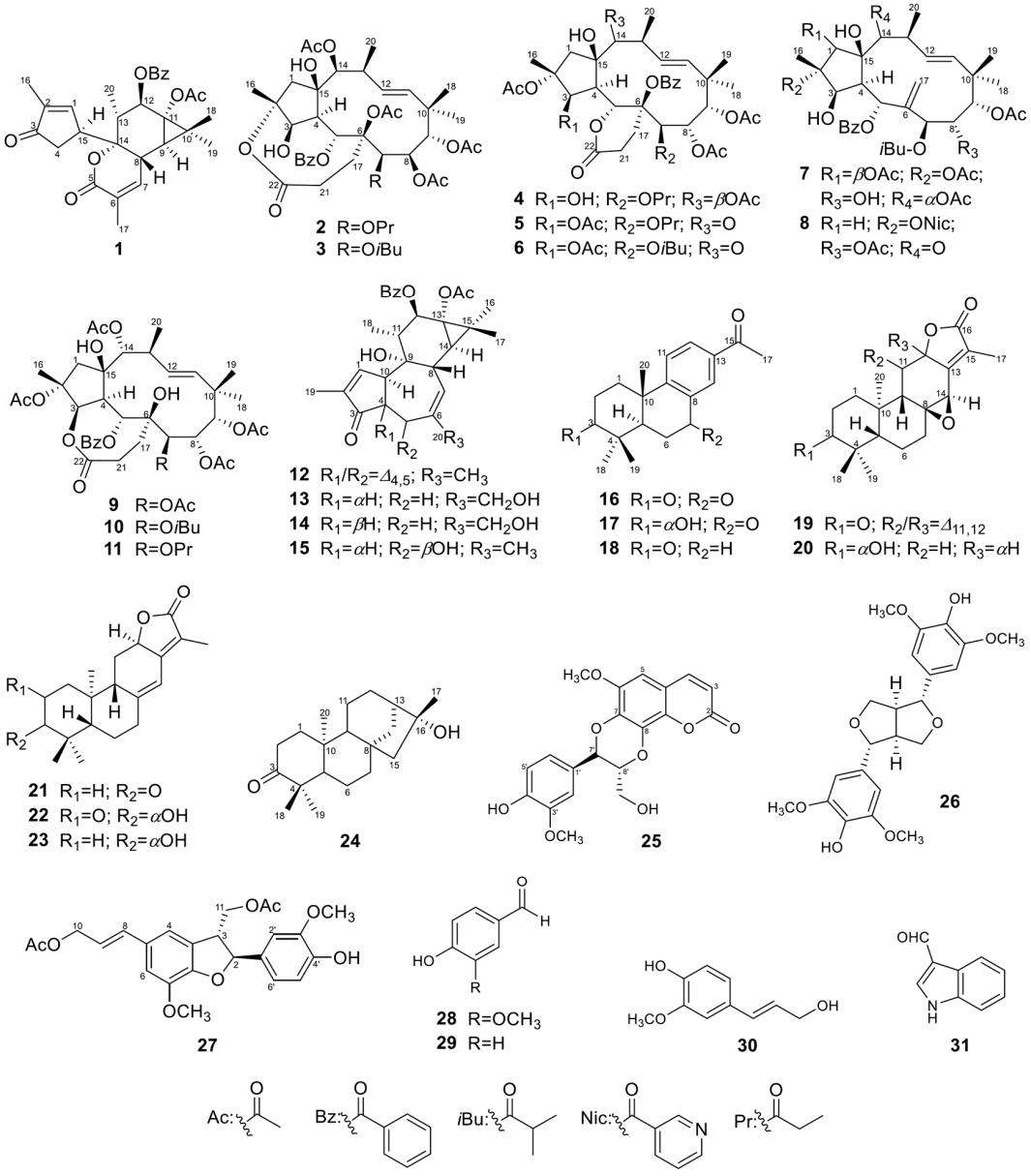

Figure 2. Structures of compounds **1**–**31** isolated from *E. usambarica*.

2.1.1. Euphordraculoate C (**1**)

Compound **1** was purified as a colorless gum with $[\alpha]_D^{28}$ −63 (*c* 0.05, $CHCl_3$). The molecular formula was identified as $C_{29}H_{32}O_7$ by HR-ESIMS *m/z* 493.2237 $[M + H]^+$ (calcd. for $C_{29}H_{33}O_7$ 493.2221), indicating 14 unsaturated degrees. The ^1H NMR spectrum of **1** revealed six methyls, an oxygenated methine, two unsaturated methines, and a mono-substituted aromatic group (Table 1). The ^{13}C-JMOD spectrum of **1** evidenced 29 carbon signals, including six methyls, one methylene, seven olefinic methines, one oxygenated methine, four saturated methines, one quaternary, three olefinic quaternary, two oxygenated quaternary, and four carbonyl carbons (Table 2). According to the combination of the 1D and 2D NMR spectra, one benzoyloxy group (OBz) [δ_H 8.02 (2H), 7.58, 7.46 (2H); δ_C 166.2, 133.2, 130.4, 129.9 (2C), 128.6 (2C)] and one acetoxy (OAc) (δ_H 1.97; δ_C 170.4, 21.1) could be identified in **1**. Based on the COSY and HSQC spectra of **1**, a series of COSY correlations between an olefinic methine (δ_H 7.52, CH-1)/a methine (δ_H 3.80, CH-15)/methylene (δ_H 2.52, 2.24, CH_2-4), together with the allylic four-bond coupling between H-1 and a methyl group [δ_H 1.74 (3H), CH_3-16]. Key HMBC correlations from H-1 and H-16 to an olefinic quaternary carbon C-2 (δ_C 141.3) and a ketone carbon C-3 (δ_C 206.8), and H-4 to C-3, indicated the presence of an *α*-methyl-*α*,*β*-unsaturated cyclopentanone moiety. Moreover, a series of COSY correlations between a methine (δ_H 2.37, CH-8), an olefinic methine (δ_H 6.68, CH-7), and an allylic coupled methyl group [δ_H 2.02 (3H), CH_3-17], together with the key HMBC correlations from H-7 to a carbonyl carbon C-5 (δ_C 163.4) and an oxygenated quaternary carbon C-14 (δ_C 85.8), H-8 to an olefinic quaternary carbon C-6 (δ_C 127.8), and H_3-17 to C-5, C-6, and C-7, indicated the presence of an *α*-methyl-*α*,*β*-unsaturated-*δ*-lactone moiety. A *gem*-dimethylcyclopropane moiety could be identified by the key HMBC correlations from two methyl groups [δ_H 1.43 (3H), δ_C 16.5, CH_3-18; δ_H 1.16 (3H), δ_C 24.8, CH_3-19] to a methine C-9 (δ_H 1.02, δ_C 34.0), a quaternary carbon C-10 (δ_C 24.9), an oxygenated quaternary carbon C-11 (δ_C 63.4) and each other, and H-9 to C-10 and C-11. In addition, the ^1H–^1H COSY cross peak between H-8/H-9, a methyl group [δ_H 0.91 (3H), CH_3-20]/a methine (δ_H 2.10, CH-13)/an oxygenated methine (δ_H 5.86, CH-12), as well as the HMBC correlations from H-7 to C-14, H-8 to C-11 and C-13, H-9 to C-11 and C-14, H-12 to C-10 and C-11, and C-13 to C-14, demonstrated the presence of a six-membered ring fusion with the *gem*-dimethyl-cyclopropane moiety at C-9 and C-11, and the *α*-methyl-*α*,*β*-unsaturated-*δ*-lactone moiety at C-8 and C-14. The HMBC correlations from H-4 to C-14 and H-8 to C-15 indicated that the *α*-methyl-*α*,*β*-unsaturated cyclopentanone moiety was linked to C-14. The OAc and OBz groups should be connected to C-11 and C-12, respectively, based on HMBC correlations (Figure 3). Additionally, comparing the NMR data of **1** with those of euphordraculoate A [34] suggested the same rare diterpenoid skeleton of both compounds. According to the NOESY cross-peaks between H-8/H-13, H-8/H_3-18, H-8/H-15, H-9/H_3-19, 11-OAc/H_3-19, H-12/H_3-20, and H-13/H_3-18, as well as comparing with euphordraculoate A [34] and euphodendriane A [35], the relative configuration of **1** was established as shown on structural formula (Figure 3), and the compound was named as euphordraculoate C.

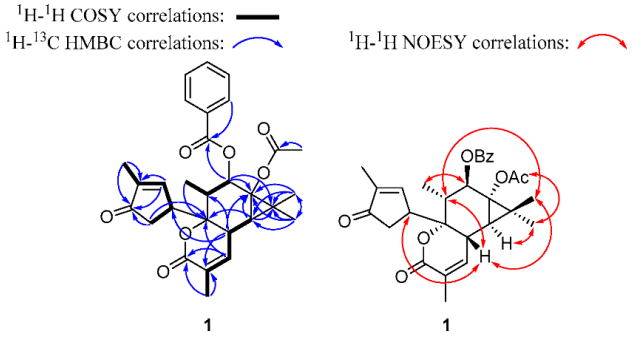

Figure 3. The ^1H-^1H COSY, key HMBC, and NOESY correlations of compound **1**.

Table 1. ^{1}H NMR data of compounds **1–6** in $CDCl_3$ at 500 MHz (δ_H in ppm, mult. *J* in Hz).

Position	1	2	3	4	5	6
1	7.52, br s	a: 2.87, d (16.5) b: 2.09, d (16.5)	a: 2.89, d (17.0) b: 2.08, d (17.0)	a: 2.87, d (16.5) b: 2.18, d (16.5)	a: 2.76, d (16.0) b: 2.04, d (16.0)	a: 2.75, d (16.0) b: 2.06, d (16.0)
3		4.26, dd (9.5, 3.5)	4.25, dd (9.5, 3.5)	4.52, dd (12.5, 4.0)	5.80, dd (4.5, 1.0)	5.82, dd (4.0, 1.0)
4	a: 2.52, dd (18.5, 6.5) b: 2.24, dd (18.5, 3.5)	2.53, m	2.54, m	2.63, m	3.92, m	3.92, m
5		6.53, d (2.0)	6.55, d (2.0)	6.09, m	5.70, d (10.0)	5.70, d (10.0)
7	6.68, dd (6.5, 1.5)	5.39, s	5.38, s	5.40, s	6.39, s	6.39, s
8	2.37, br d (6.5)	5.73, d (4.5)	5.75, d (4.5)	5.77, d (5.0)	5.72, s	5.75, s
9	1.02, d (2.0)	4.88, d (4.5)	4.91, d (4.5)	4.83, d (5.0)	4.99, s	5.01, s
11		5.49, d (16.0)	5.48, d (16.0)	5.41, d (16.0)	6.16, d (16.0)	6.16, d (16.0)
12	5.86, d (10.5)	5.83, dd (16.0, 10.0)	5.85, dd (16.0, 9.5)	5.72, dd (16.0, 10.0)	5.43, dd (16.0, 10.0)	5.41, dd (16.0, 10.0)
13	2.10, dq (10.5, 6.5)	2.46, m	2.46, m	2.55, m	3.97, m	3.98, m
14		4.89, s	4.89, s	5.18, s		
15	3.80, m					
16	1.74, dd (2.5, 1.5)	1.73, s	1.73, s	1.72, s	1.56, s	1.57, s
17	2.02, br s	a: 3.31, m b: 2.12, m	a: 3.33, m b: 2.06, m	a: 3.09, ddd (15.5, 7.5, 2.5) b: 2.40, m	a: 2.72, m b: 2.01, m	a: 2.69, m b: 1.98, m
18	1.43, s	0.93, s	0.93, s	0.93, s	0.98, s	0.97, s
19	1.16, s	1.13, s	1.12, s	0.96, s	1.44, s	1.43, s
20	0.91, d (6.5)	1.14, d (6.5)	1.14, d (7.0)	1.15, d (7.0)	1.23, d (7.0)	1.23, d (6.5)
21		a: 2.36, m b: 2.27, m	a: 2.35, dd (11.5, 7.5) b: 2.28, dd (11.5, 5.0)	a: 2.65, m b: 2.16, m	a: 3.43, m b: 2.50, m	a: 3.53, m b: 2.52, m
2-OAc				2.13, s	2.26, s	2.27, s
3-OAc					2.05, s	2.05, s
3-OH		3.45, d (9.5)	3.44, d (9.5)	3.03, d (12.5)		
5-OBz		7.93, m 7.52, m 7.39, m	7.93, m 7.53, m 7.39, m			
6-OAc		2.14, s	2.15, s			
6-OBz				7.92, m 7.58, m 7.41, m	7.88, m 7.65, m 7.51, m	7.90, m 7.67, m 7.51, m
7-O*i*Bu			2.61, h (7.0) 1.21, d (7.0) 1.20, d (7.0)			2.63, h (7.0) 1.26, d (7.0) 1.22, d (7.0)
7-OPr		2.41, q (7.5) 1.16, t (7.5)		2.57, m 2.50, m 1.22, t (7.5)	2.49, m 2.31, m 1.23, m	
8-OAc		2.08, s	2.09, s	1.35, s	2.00, s	2.02, s
9-OAc		2.17, s	2.17, s	2.07, s	2.03, s	2.07, s
11-OAc	1.97, s					
12-OBz	8.02, dd (8.5, 1.5) 7.58, m 7.46, dd (8.5, 7.5)					
14-OAc		2.56, s	2.56, s	2.45, s		
15-OH		3.07, s	3.05, s	4.61, s	4.04, s	4.08, s

Table 2. ^{13}C NMR data of compounds **1–6** in $CDCl_3$ at 125 MHz (δ_C in ppm).

Position	1	2	3	4	5	6
1	160.2	49.1	49	45.7	52.5	52.5
2	141.3	89.5	89.5	90.1	87.7	87.7
3	206.8	80.5	80.4	80.7	80	79.8
4	37.9	43.3	43.1	44.9	45.2	45.1
5	163.4	72.8	73.1	85	73.2	72.9
6	127.8	92.5	92.4	84.4	81.1	81.6
7	141.4	70.8	70.5	69.1 [e]	68.2	68.1
8	35.2	68.9	69	69.2 [e]	68.1	68.1
9	34	79.4	78.9	78.8	81.7	81.7
10	24.9	41.2	41.2	40.6	40.3	40.4
11	63.4	134.6	134.6	135.3	137.4	137.3
12	76.2	133	132.9	134.1	128.9	128.9
13	38.9	37.4	37.4	39	43.9	43.6
14	85.8	81.6	81.5	82.2	211.4	211.6

Table 2. *Cont.*

Position	1	2	3	4	5	6
15	45.8	86.3	86.3	87.1	84.6	84.6
16	10.2	19.1	19	20	18.5	18.5
17	17.4	24.5	24	23.4	26.5	26.6
18	16.5	26	26	26.8	25.8	26
19	24.8	21.7 [a]	21.2 [c]	21.9	23.2	23.1
20	12.5	23.2	23.1	22.4	21.7	21.6
21		26	28.3	26	29.1	29.2
22		175.1	174.9	168.1	172.7	172.7
2-OAc				169.7 [f], 22.7	169.6 [g], 22.4	169.6 [i], 22.4
3-OAc					169.1 [g], 20.6 [h]	169.2 [i], 21.0 [j]
5-OBz		164.5, 133.5, 129.7, 129.6, 128.8	164.3, 133.3, 129.6, 129.5, 128.7			
6-OAc		169.8, 21.5 [a]	169.6 [d], 21.6			
6-OBz				163.9, 133.8 130.1, 130.0 128.7	165.8, 133.81 30.6, 129.7 128.5	166.0, 133.8 130.7, 129.7 128.5
7-O*i*Bu			176.4, 34.2 18.8, 18.5			175.2, 34.5 19.0, 18.1
7-OPr		174.2 [b], 27.7, 8.9		174.6, 27.5, 8.9	173.4, 27.6, 8.6	
8-OAc		170, 21.6 [a]	169.9 [d], 21.4 [c]	169.9 [f], 21.0	170.0 [g], 21.2 [h]	170.0 [i], 21.1 [j]
9-OAc		170.2, 22.7	169.8 [d], 22.6	169.8 [f], 21.5	169.9 [g], 20.9 [h]	170.1 [i], 20.9 [j]
11-OAc	170.4, 21.1					
12-OBz	166.2, 133.2 130.4, 129.9 128.6					
14-OAc		174.3 [b], 21.4 [a]	174.3, 21.3 [c]	170.8, 20.8		

[a–j]: Exchangeable.

2.1.2. Usambariphane A (**2**)

Compound **2** was obtained as a white amorphous powder. Its molecular formula was calculated as $C_{40}H_{52}O_{16}$ by the analysis of HR-ESIMS *m/z* 789.3327 $[M + H]^+$ (calcd. for $C_{40}H_{53}O_{16}$ 789.3328). The NMR spectra of **2** revealed clearly four OAc (δ_H 2.56, δ_C 174.3, 21.4; δ_H 2.17, δ_C 170.2, 22.7; δ_H 2.14, δ_C 169.8, 21.5; δ_H 2.08, δ_C 170.0, 21.6), one OBz (δ_H 7.93 (2H), 7.52, 7.39 (2H), δ_C 164.5, 133.5, 129.7, 129.6, 128.8), one propionate group [δ_H 2.41 (2H), 1.16 (3H), δ_C 174.2, 27.7, 8.9; OPr], four methyls [δ_H 1.73 (3H), δ_C 19.1, CH_3-16; δ_H 0.93 (3H), δ_C 26.0, CH_3-18; δ_H 1.13 (3H), δ_C 21.7, CH_3-19; δ_H 1.14 (3H), δ_C 23.2, CH_3-20], a *trans*-disubstituted C=C (δ_H 5.49, δ_C 134.6, CH-11; δ_H 5.83, δ_C 133.0, CH-12), and a lactone carbonyl carbon (δ_C 175.1, C-22). Further, comparing the 1D NMR data of **2** (Tables 1 and 2) with those of isoterracinolide A (**10**) [36], the skeleton of **2** was established as a dihomojatrophane type diterpenoid [7] with a double bond at $\Delta_{11,12}$ and a lactone moiety. An OH group was located at C-3 based on a ^1H–^1H COSY cross peak between H-3 and 3-OH, as well as the HBMC correlations from 3-OH to C-3 and C-4. Another OH group was connected to C-15 by the confirmation of the HMBC correlations from 15-OH to C-4, C-14, and C-15. Moreover, the HMBC correlations from H-5 to δ_C 164.5, H-7 to δ_C 174.2, H-8 to δ_C 170.0, H-9 to δ_C 170.2, H-14 to δ_C 174.3, indicated that OBz and OPr were located at C-5 and C-7 respectively, and three OAc were linked to C-8, C-9, and C-14 each. The last OAc was located apparently to C-6 based on NOESY correlations between the acetyl proton signal δ_H 2.14 (6-OAc) with H-5 and H-17a. The remaining lactone ring was proposed to be constructed between C-17 and C-2 in structure **2**. According to the ^{13}C signal value of C-6 (δ_C 92.5) of **2** was close to the signal in sororianolide A (δ_C 93.0, C-6-βOAc) and different from sororianolide B (δ_C 80.9, C-6-αOAc), suggesting the OAc at C-6 in **2** can be assigned as β-oriented [37]. Moreover, the NOESY correlations of H-3/H_2-17, H-3/H-4, H-4/H-7, H-4/H-8, H-8/H_3-19, H_3-19/H-13, H_3-19/H-14, H_3-16/3-OH, H_3-16/H-1b, H-1b/15-OH, 15-OH/H-9, and H-9/H_3-18 indicted the configurations of 3β-OH, Hα-4, Hβ-5, 6β-OAc, 7β-OPr, 8β-OAc, 9α-OAc, 14β-OAc, 15-βOH, βCH_3-16, and βCH_3-20. Thus, the structure of **2** was established and named as usambariphane A.

2.1.3. Usambariphane B (**3**)

Compound **3** was obtained as a white amorphous powder. The molecular formula was determined as $C_{41}H_{54}O_{16}$ based on HR-ESIMS m/z 803.3488 $[M + H]^+$ (calcd. for $C_{41}H_{55}O_{16}$ 803.3485). The 1D NMR data (Tables 1 and 2) of 3 were highly similar to those of 2, except for an isobutyryl group (OiBu) [δ_H 2.61, 1.21 (3H), 1.20 (3H), δ_C 176.4, 34.2, 18.8, 18.5] instead of propanoyl. The isobutyryl group was connected to C-7 in 3 based on the HMBC correlation from H-7 (δ_H 5.38) to the OiBu carbonyl carbon (δ_C 176.4). The NOESY correlations of 3 revealed the same relative configuration as that of 2. The structure of 3 was established and named as usambariphane B.

2.1.4. Usambariphane C (**4**)

Compound **4** was purified as a colorless crystal. The molecular formula was identified as $C_{40}H_{52}O_{16}$ by HR-ESIMS *m/z* 789.3346 $[M + H]^+$ (calcd. for $C_{40}H_{53}O_{16}$ 789.3328). Based on the comparison of the ^1H and ^{13}C NMR data (Tables 1 and 2) for **4** with those of usambariphane B (**2**), the skeleton of **4** was suggested to be a C_{22} dihomojatrophane with a double bond at $\Delta_{11,12}$ (δ_H 5.41, δ_C 135.3, CH-11; δ_H 5.72, δ_C 134.1, CH-12) and a lactone moiety (δ_H 3.09, 2.40, δ_C 23.4, CH_2-17; δ_H 2.65, 2.16, δ_C 26.0, CH_2-21; δ_C 168.1, C-22). A δ-lactone ring was constructed at C-5 and C-6 supporting by the ^1H–^1H COSY cross peak between H_2-17 and H_2-21, as well as the HMBC correlations from H-5 to C-17 and C-22, H_2-17 to C-5, C-6, and C-22, and H_2-21 to C-6 and C-22. Moreover, the 1D NMR data of **4** were highly close to those of euphosorophane D [38] except for an OPr group [δ_H 2.57, 2.50, 1.22 (3H); δ_C 174.6, 27.5, 8.9] at C-7 according to an HMBC correlation from H-7 (δ_H 5.40) to δ_C 174.6. The NOESY cross-peaks of **4** demonstrated the same relative orientations to those of euphosorophane D [38]. Therefore, the structure of **4** was established and named as usambariphane C.

2.1.5. Usambariphane D (**5**)

Compound **5** was purified as a colorless crystal. The molecular formula was identified as $C_{40}H_{50}O_{16}$ by HR-ESIMS *m/z* 787.3193 $[M + H]^+$ (calcd. for $C_{40}H_{51}O_{16}$ 787.3172). The inspection of 1D (Tables 1 and 2) and 2D NMR data suggested that compound **5** was a bishomojatrophane type diterpenoid with a double bond at $\Delta_{11,12}$ (δ_H 6.16, δ_C 137.4, CH-11; δ_H 5.43, δ_C 128.9, CH-12), a lactone moiety (δ_H 2.72, 2.01, δ_C 26.5, CH_2-17; δ_H 3.43, 2.50, δ_C 29.1, CH_2-21; δ_C 172.7, C-22), and a ketone unit δ_C 211.4 (C-14). A δ-lactone ring was constructed at C-5 and C-6 supporting by the ^1H–^1H COSY cross peak between H_2-17 and H_2-21, and the HMBC correlations from H-5 to C-17 and C-22, H_2-17 to C-5, C-6, and C-22, and H_2-21 to C-6 and C-22. The ketone unit in **5** was located at C-14 based on the HMBC correlations from H-1, H-12, H-13, and H_3-20 to C-14, respectively. An OH group was connected to C-15 by the confirmation of HMBC correlations from 15-OH to C-4, C-14, and C-15. Moreover, four OAc [δ_H 2.26 (3H), δ_C 169.6, 22.4; δ_H 2.05 (3H), δ_C 169.1, 20.6; δ_H 2.03 (3H), δ_C 169.9, 20.9; δ_H 2.00 (3H), δ_C 170.0, 21.2], one OBz [δ_H 7.88 (2H), 7.65, 7.51 (2H), δ_C 165.8, 133.8, 130.6, 129.7 (2C), 128.5 (2C)], and one OPr [δ_H 2.49, 2.31, 1.23 (3H), δ_C 173.4, 27.6, 8.6] moieties were identified clearly by the examination of the NMR spectra. The HMBC correlations from H-3 to δ_C 169.1, H-7 to δ_C 173.4, H-8 to δ_C 170.0, and H-9 to δ_C 169.9, indicated the OPr was located at C-7, and three OAc were linked to C-3, C-8, and C-9, respectively. The location of the OBz at C-6 was confirmed by the NOESY correlations between the benzoyl proton signal δ_H 7.88 with H-5, H-8, and H-12. The last OAc was connected to C-2 based on the NOE cross-peak between the acetyl proton signal δ_H 2.26 with H_3-16. The relative configuration of **5** was evaluated by the NOESY spectrum and comparison with a similar structure terracinolide J [39] to assign 2α-OAc, 3β-OAc, Hα-4, Hβ-5, 6β-OBz, 7β-OPr, 8α-OAc, 9α-OAc, βCH_3-20, and 15-βOH. Above all, the structure of **5** was established and named as usambariphane D.

2.1.6. Usambariphane E (**6**)

Compound **6** was obtained as a colorless crystal. The molecular formula was identified as $C_{41}H_{52}O_{16}$ by HR-ESIMS *m/z* 801.3356 $[M + H]^+$ (calcd. for $C_{41}H_{53}O_{16}$ 801.3328). The 1D (Tables 1 and 2) and 2D NMR data of **6** were almost identical with those of **5**, except for the ester group at C-7. In **6**, an O*i*Bu [δ_H 2.63, 1.26 (3H), 1.22 (3H), δ_C 175.2, 34.5, 19.0, 18.1] was presented at C-7 as confirmed by the HMBC correlation from H-7 (δ_H 6.39) to δ_C 175.2. The NOESY correlations of **6** revealed the same relative configuration as that of **5**. The structure of **6** was established and named as usambariphane E.

2.1.7. Usambariphane F (**7**)

Compound **7** was obtained as a colorless crystal. The molecular formula was identified as $C_{39}H_{52}O_{15}$ by HR-ESIMS *m/z* 761.3383 $[M + H]^+$ (calcd. for $C_{39}H_{53}O_{15}$ 761.3379). The 1D (Table 3) and 2D NMR spectra of **7** revealed four OAc [δ_H 2.24 (3H), δ_C 170.1, 21.0; δ_H 2.12 (3H), δ_C 170.9, 22.5; δ_H 2.06 (3H), δ_C 172.1, 20.9; δ_H 1.70 (3H), δ_C 172.2, 20.4], one O*i*Bu [δ_H 2.55, 1.19 (3H), 1.14 (3H), δ_C 175.1, 34.0 19.6, 18.4], one OBz [δ_H 8.00 (2H), 7.56, 7.42 (2H), δ_C 165.4, 133.4, 130.1, 129.7 (2C), 128.8 (2C)], four methyls [δ_H 1.55 (3H), δ_C 17.1, CH_3-16; δ_H 1.03 (3H), δ_C 27.6, CH_3-18; δ_H 1.40 (3H), δ_C 23.4, CH_3-19; δ_H 1.06 (3H), δ_C 23.9, CH_3-20], a *trans*-disubstituted C=C (δ_H 5.93, δ_C 134.0, CH-11; δ_H 5.76, δ_C 130.9, CH-12), and an exocyclic methylene (δ_H 5.26, 5.10, δ_C 110.4, CH_2-17). Further, the skeleton of **7** was established as a jatrophane type diterpenoid with two double bonds at $\Delta_{6,17}$ and $\Delta_{11,12}$ based on the series ^1H–^1H COSY correlations of H-3/H-4/H-5 and H-11/H-12/H-13/H-14 and H_3-20, as well as the HMBC correlations from H-1 to C-2 and C-16, H-3 to C-1, C-2, C-4 and C-15, and H_3-16 to C-1, C-2 and C-3, H-5 to C-3, C-4, C-6, C-15, C-17, H-7 to C-6 and C-9, H-8 to C-6 and C-10, H-9 to C-8 and C-11, H-11 to C-10 and C-13, H-12 to C-10, H-14 to C-1, C-4, C-12, C-13, and C-15, H_2-17 to C-5, C-6, and C-7, H_3-18 and H_3-19 to C-9, C-10 and C-11, H_3-20 to C-12, C-13, and C-14. The presence of the 3-OH group was deduced by the ^1H–^1H COSY cross-peak between H-3 and 3-OH, and the HMBC correlations from 3-OH to C-2, C-3, and C-4. Another OH group was located at C-8 by the COSY cross-peak between H-8 and 8-OH, and the HMBC correlations from 8-OH to C-7 and C-8. The third OH group was connected to C-15 by the confirmation of the HMBC correlations from 15-OH to C-1, C-4, and C-15. The HMBC correlations of H-1/δ_C 170.1 (OAc), H-5/δ_C 165.4 (OBz), H-7/δ_C 175.1 (O*i*Bu), H-9/δ_C 172.1 (OAc), and H-14/δ_C 172.2 (OAc), demonstrated the locations of the acyl groups, and of necessity, the last OAc was located at C-2. The relative configuration of **7** was deduced by the NOESY spectrum. The H-4 and 15-OH in **7** can be assigned as α- and β-oriented, respectively, according to the comparison of the NMR data with those of known jatrophane-type diterpenoids [38,40]. The NOESY cross-peaks of H-1/H-4, H-3/H-4, and H-4/H-7 indicated the α-orientation of H-1, H-3, and H-7; meanwhile, the NOESY cross-peaks of H-5/15-OH, H-5/H-8, H-8/H_3-19, H-9/H_3-19, H-14/15-OH and H-14/H_3-20 indicated the β-orientation of H-5, H-8, H-9, H-14, H_3-19, and H_3-20. Above all, the structure of **7** was established and named as usambariphane F.

2.1.8. Usambariphane G (**8**)

Compound **8** was obtained as a colorless crystal. The molecular formula was identified as $C_{41}H_{49}O_{13}N$ by HR-ESIMS *m/z* 764.3230 $[M + H]^+$ (calcd. for $C_{41}H_{50}O_{13}N$ 764.3277), indicating 18 degrees of molecular unsaturation. The 1D (Table 3) and 2D NMR spectra of **8** revealed two OAc [δ_H 2.07 (3H), δ_C 169.7, 20.7; δ_H 2.00 (3H), δ_C 169.9, 20.8], an O*i*Bu [δ_H 2.60, 1.23 (3H), 1.11 (3H), δ_C 175.8, 34.0 19.7, 18.4], an OBz [δ_H 8.06 (2H), 7.56, 7.44 (2H), δ_C 164.7, 133.4, 131.1, 130.0 (2C), 128.7 (2C)], a nicotinate group [δ_H 9.41, 8.79, 8.52, 7.39, δ_C 164.9, 153.4, 151.5, 137.6, 127.5, 123.2; ONic], four methyls [(δ_H 1.89 (3H), δ_C 20.9, CH_3-16; δ_H 0.91 (3H), δ_C 26.5, CH_3-18; δ_H 1.36 (3H), δ_C 23.2, CH_3-19; δ_H 1.24 (3H), δ_C 19.6, CH_3-20)], a *trans*-disubstituted C=C (δ_H 5.87, δ_C 137.9, CH-11; δ_H 5.57, δ_C 129.6, CH-12), ketone unit (δ_C 211.2, C-14), and an exocyclic methylene (δ_H 5.41, 5.16, δ_C 111.6, CH_2-17). The skeleton of **8** was established as a jatrophane-type diterpenoid with two double bonds at $\Delta_{6,17}$ and

$\Delta_{11,12}$, and the ketone unit at C-14 based on the series ^{1}H–^{1}H COSY correlations of H-3 (δ_H 4.76)/H-4 (δ_H 3.32)/H-5 (δ_H 5.67) and H-11/H-12/H-13 (δ_H 3.75)/H_3-20; and the HMBC correlations from H_2-1 (δ_H 2.95 and 2.27) to C-4 (δ_C 47.9), C-14, and C-15 (δ_C 89.0), H-3 to C-1(δ_C 51.4), C-2 (δ_C 92.0) and C-15, H-4 to C-15, H_3-16 to C-1, C-2 and C-3 (δ_C 79.1), H-5 to C-3, C-6 (δ_C 144.9), and C-7 (δ_C 68.5), H-8 (δ_H 5.18) to C-6, C-7, C-9 (δ_C 80.6), and C-10 (δ_C 41.1), H-9 (δ_H 4.96) to C-10 and C-11, H-11 to C-9, C-10, C-13 (δ_C 44.4), C-18, and C-19, H-12 to C-10, H-13 to C-11, C-12, and C-14, H_2-17 to C-5, C-6, and C-7, H_3-18 and H_3-19 to C-9 and C-10, H_3-20 to C-12, C-13, and C-14. An OH group was located at C-3 based on a ^{1}H–^{1}H COSY cross-peak between H-3 and 3-OH (δ_H 3.57), and the HMBC correlations from 3-OH to C-3 and C-4. Another OH group was connected to C-15 by the confirmation of the HMBC correlations from 15-OH (δ_H 4.34) to C-1, C-4, and C-15. Furthermore, the HMBC correlations of H-5/δ_C 164.7 (OBz), H-7/δ_C 175.8 (O*i*Bu), H-8/δ_C 169.9 (OAc), H-9/δ_C 169.7 (OAc), demonstrated the locations of these acyl groups, and thereby the ONic was located at C-2. According to the NOESY cross-peaks of H-1a/H-4, H-1a/H-13, H-3/H-4, H-4/H-7, H-4/H-13, H-5/H-8, H-5/15-OH, H-8/H_3-19, H-9/H_3-19, H_3-19/H_3-20, 3-OH/15-OH, 3-OH/H_3-16, and comparison of the NMR data with those of (2*R*,3*R*,4*R*,5*R*,7*S*,8*S*,9*S*,11*E*, 13*S*,15*R*)-2,3,5,7,8,9,15-heptahydroxyjatropha-6(17),11-diene-14-one-2,3,8,9-tetraacetate-5-benzoate-7-(2-methylpropionate) [41] indicated the relative configuration of **8** as depicted on Figure 2. The structure of **8** was established and named as usambariphane G.

Table 3. ^{1}H (500 MHz) and ^{13}C (125 MHz) NMR data of compounds **7**–**9** in $CDCl_3$ (δ in ppm).

Position	**7**		**8**		**9**	
	δ_H, mult. (*J* in Hz)	**δ_C**	**δ_H, mult. (*J* in Hz)**	**δ_C**	**δ_H, mult. (*J* in Hz)**	**δ_C**
1	5.46, s	79.8	a: 2.95, d (15.5) b: 2.27, d (15.5)	51.4	a: 2.83, d (16.5) b: 2.24, d (16.5)	52.0
2		90.6		92.0		88.8
3	4.36, dd (10.5, 5.5)	78.0	4.67, dd (10.0, 4.5)	79.1	5.48, d (4.0)	84.7
4	2.76, m	41.4	3.32, m	47.9	2.97, dd (4.0, 3.5)	44.2
5	6.00, br s	71.0	5.67, br s	69.2	6.58, d (3.5)	77.9
6		144.4		144.9		81.8
7	5.21, s	68.8	5.41, br s	68.5	5.27, s	68.4
8	4.30, d (11.0)	70.2	5.18, s	70.7	5.71, d (6.5)	70.0
9	4.79, s	86.6	4.96, s	80.6	4.96, d (6.5)	78.4
10		40.1		41.1		40.7
11	5.93, d (16.5)	134.0	5.87, d (15.5)	137.6	5.50, d (16.0)	134.7
12	5.76, d (16.5)	130.9	5.57, dd (15.5, 9.5)	129.6	5.79, d (16.0)	134.1
13	2.76, m	36.9	3.75	44.4	2.69, m	36.9
14	4.78, s	76.9		211.2	5.04, s	80.4
15		84.8		89.0		85.4
16	1.55, s	17.1	1.89, s	20.9	1.75, s	19.8
17	a: 5.26, s; b: 5.10, s	110.4	a: 5.41, s; b: 5.16, s	111.6	a: 1.85, m; b: 1.73, m	32.0
18	1.03, s	27.6	0.91, s	26.5	0.98, s	26.4
19	1.40, s	23.4	1.36, s	23.2	1.04, s	20.8 [e]
20	1.06, d (7.0)	23.9	1.24, d (6.5)	19.6	1.11, d (7.0)	22.4
21					a: 3.21, m; b: 2.33, m	28.1
22						173.5
1-OAc	2.24, s	170.1, 21.0 [a]				
2-OAc	2.12, s	170.9, 22.5			2.19, s	169.6, 22.9
2-ONic			9.41, dd (2.0, 1.0) 8.79, dd (5.0, 2.0) 8.52, m; 7.39, m	164.9, 153.4 151.5, 137.6 127.5, 123.2		
3-OH	3.36, d (10.5)		3.57, d (10.0)			
5-OBz	8.00, m 7.56, m 7.42, m	165.4, 133.4 130.1, 129.7 128.8	8.06, m 7.56, m 7.44, m	164.7, 133.4 131.1, 130.0 128.7	8.07, m 7.57, m 7.46, m	168.3, 133.9 130.1, 128.8 128.6
6-OH					3.57, s	
7-OAc					2.14, s	171.0, 20.9 [e]
7-O*i*Bu	2.55, h (7.0) 1.19, d (7.0) 1.14, d (7.0)	175.1, 34.0 19.6, 18.4	2.60, h (7.0) 1.23, d (7.0) 1.11, d (7.0)	175.8, 34.0 19.7, 18.4		
8-OAc			2.00, s	169.9 [c], 20.8 [d]	2.15, s	171.2, 21.7 [f]
8-OH	3.15, d (11.0)					
9-OAc	2.06, s	172.1 [b], 20.9 [a]	2.07, s	169.7 [c], 20.7 [d]	2.16, s	170.4, 21.4 [f]
14-OAc	1.70, s	172.2 [b], 20.4			2.36, s	172.0, 20.7 [e]
15-OH	2.75, s		4.34, s		2.40, s	

[a–f]: Exchangeable.

2.1.9. Isoterracinolides C (**9**)

Compound **9** was obtained as a white amorphous powder with a molecular formula of $C_{39}H_{50}O_{16}$ determined based on HR-ESIMS *m/z* 775.3172 $[M + H]^+$ (calcd. for $C_{39}H_{51}O_{16}$ 775.3172). The 1D (Table 3) and 2D NMR spectra of **9** revealed five OAc [δ_H 2.36 (3H), δ_C 172.0, 20.7; δ_H 2.19 (3H), δ_C 169.6, 22.9; δ_H 2.16 (3H), δ_C 170.4, 21.4; δ_H 2.15 (3H), δ_C 171.2, 21.7; δ_H 2.14 (3H), δ_C 171.0, 20.9], one OBz [δ_H 8.07 (2H), 7.57, 7.46 (2H), δ_C 168.3, 133.9, 130.1 (2C), 128.8 (2C), 128.6], four methyls [δ_H 1.75 (3H), δ_C 19.8, CH_3-16; δ_H 0.98 (3H), δ_C 26.4, CH_3-18; δ_H 1.04 (3H), δ_C 20.8, CH_3-19; δ_H 1.11 (3H), δ_C 22.4, CH_3-20], and a *trans*-disubstituted C=C (δ_H 5.50, δ_C 134.7, CH-11; δ_H 5.79, δ_C 134.1, CH-12), and a lactone carbonyl carbon (δ_C 173.5, C-22). Further, comparing the NMR data of **9** with those of isoterracinolide A (**10**) [36] indicated that the structure of **9** is very similarly to **10**, except for the O*i*Bu which was replaced in **10** by an OAc. The HMBC correlation from H-7 to δ_C 171.0 suggested that the OAc was located at C-7 in **9**. Compound **9** was thus established and named as isoterracinolides C.

2.1.10. 4β-Crotignoid K (**14**)

Compound **14** was obtained as a white amorphous powder. The molecular formula was determined as $C_{29}H_{34}O_7$ by HR-ESIMS *m/z* 495.2385 $[M + H]^+$ (calcd. for $C_{29}H_{35}O_7$ 495.2377). The 1D (Tables 4 and 5) and 2D NMR of **14** revealed one OAc [δ_H 2.14 (3H), δ_C 173.9, 21.3], one OBz [δ_H 8.02 (2H), 7.59, 7.47 (2H), δ_C 166.4, 133.4, 130.1, 129.9 (2C), 128.7 (2C)], four methyls [δ_H 1.21 (3H), δ_C 23.9, CH_3-16; δ_H 1.33 (3H), δ_C 17.1, CH_3-17; δ_H 0.98 (3H), δ_C 15.3, CH_3-18; δ_H 1.73 (3H), δ_C 10.3, CH_3-19], an oxygenated methylene [δ_H 4.05 (2H), δ_C 67.6, CH_2-20], an oxygenated methine (δ_H 5.68, δ_C 77.8, CH-12), two unsaturated methines (δ_H 7.57, δ_C 159.7, CH-1; δ_H 5.56, δ_C 126.6, CH-7), and a ketone unit (δ_C 208.7, C-3). The interpretation of HMBC correlations suggested the skeleton of **14** was a tigliane-type diterpenoid [7] with an *α*-methyl-*α*,*β*-unsaturated cyclopentanone ring fused between C-4 and C-10, an OH (δ_H 5.62) connected to C-9, the OBz connected to C-12, the OAc connected to C-13 and a hydroxymethyl linked to C-6. Moreover, according to the NOESY correlations of H-4/H-8/H-11/H_3-17 and H-12/H-14/9-OH/H_3-18, as well as comparing the 1D NMR data of **14** with those of crotignoid K (**13**) [42] and 4-deoxyphorbol 12, 13-*bis*(isobutyrate) [43]. The structure of **14** was established as a 4*β* proton against the 4*α* proton of crotignoid K, thus named as 4*β*-crotignoid K.

2.1.11. Euphodendriane B (**15**)

Compound **15** was obtained as a white amorphous powder. The molecular formula was determined as $C_{29}H_{34}O_7$ by HR-ESIMS *m/z* 495.2396 $[M + H]^+$ (calcd. for $C_{29}H_{35}O_7$ 495.2377). The 1D (Tables 4 and 5) and 2D NMR of **15** revealed one OAc [δ_H 2.11 (3H), δ_C 174.1, 21.2], one OBz [δ_H 8.06 (2H), 7.61, 7.49 (2H), δ_C 166.4, 133.4, 130.1, 129.9 (2C), 128.7 (2C)], five methyls [δ_H 1.20 (3H), δ_C 24.3, CH_3-16; δ_H 1.33 (3H), δ_C 16.7, CH_3-17; δ_H 1.16 (3H), δ_C 11.9, CH_3-18; δ_H 1.83 (3H), δ_C 10.6, CH_3-19; δ_H 1.90 (3H), δ_C 27.2, CH_3-20], two oxygenated methines (δ_H 4.46, δ_C 71.1, CH-5; δ_H 5.73, δ_C 75.7, CH-12), two unsaturated methines (δ_H 7.06, δ_C 154.6, CH-1; δ_H 4.88 δ_C 125.5, CH-7), and a ketone unit (δ_C 207.5, C-3). The interpretation of HMBC correlations demonstrated that **15** was a tigliane-type diterpenoid with an *α*-methyl-*α*,*β*-unsaturated cyclopentanone ring fused between C-4 and C-10, with two OH (δ_H 5.92 and 5.95) connected to C-5 and C-9 respectively, one OBz connected to C-12, and one OAc connected to C-13 and 20-methyl group. The NMR data of **15** was highly close to those of euphodendriane A [35], except for the substitution at C-13 where an O*i*Bu in euphodendriane A was replaced in **15** by the OAc. The relative configuration of **15** was deduced by inspection of the NOESY spectrum, showing the same orientations to euphodendriane A [35]. Thus, the structure of **15** was established and named as euphodendriane B.

2.1.12. 16-Nor-abieta-8,11,13-trien-3,7,15-trione (**16**)

Compound **16** was obtained as a colorless crystal with a molecular formula of $C_{19}H_{22}O_3$ identified by HR-ESIMS *m/z* 299.1648 $[M + H]^+$ (calcd. for $C_{19}H_{22}O_3$ 299.1642). The 1D (Tables 4 and 5) and 2D NMR data of **16** revealed an acetyl moiety (δ_C 197.3, C-15; δ_H 2.64 (3H), δ_C 26.9, CH_3-17), three methyls [δ_H 1.17 (3H), δ_C 25.2, CH_3-18; δ_H 1.23 (3H), δ_C 21.7, CH_3-19; δ_H 1.48 (3H), δ_C 22.8, CH_3-20], three methylenes [δ_H 2.68, 2.05, δ_C 36.8, CH_2-1; δ_H 2.91, 2.59, δ_C 34.6, CH_2-2; δ_H 2.83, 2.75, δ_C 36.5, CH_2-6], a methine (δ_H 2.36, δ_C 49.2, CH-5), a set of trisubstituted aromatic ring (δ_C 130.8, C-8; δ_C 158.2, C-9; δ_H 7.49 (d, *J* = 8.5), δ_C 125.2, CH-11; δ_H 8.17 (dd, *J* = 8.5, 2.5), δ_C 133.4, CH-12; δ_C 135.9, C-13; δ_H 8.57 (d, *J* = 2.5), δ_C 128.3, CH-14], two ketone units (δ_C 214.0, C-3; δ_C 197.4, C-7), and two quaternary carbons (δ_C 47.6, C-4; δ_C 38.3, C-10). The HMBC correlations of **16** from H_2-1 to C-3, C-9, and C-20, H_2-2 to C-3 and C-4, H-5 to C-1, C-4, C-9, and C-10, H_2-6 to C-7, C-8, and C-10, H-12 to C-15, H-14 to C-7 and C-15, H_3-17 to C-13, H_3-18 and H_3-19 to C-3, C-4, and C-5, and H_3-20 to C-5 and C-10, suggested that **16** was an abietane-type diterpenoid [7] and was structurally similar to a known compound abieta-8,11,13-triene-3,7-dione [44,45], except for the substitution of the acetyl moiety at C-15–C-17. The relative configuration of **16** was the same as the typical abieta-8,11,13-triene diterpenoids [45] based on the NOESY correlations of H-5/H_3-18 and H_3-19/H_3-20 as well as the comparison of the NMR data of **16** with those of literature [44,45]. The structure of **16** was identified as 16-nor-abieta-8,11,13-trien-3,7,15-trione.

Table 4. ^{1}H NMR data of compounds **14**–**17**, **19**, and **20** in CDCl3 at 500 MHz (δ_H in ppm, mult. *J* in Hz).

Position	14	15	16	17	19	20
1	7.57, s	7.06, br s	a: 2.68, m b: 2.05, m	a: 2.42, m b: 1.73, m	a: 2.05, m b: 1.75, m	a: 1.98, m b: 1.24, m
2			a: 2.91, m b: 2.59, ddd (15.5, 5.5, 3.0)	a: 1.92, m b: 1.87, m	a: 2.65, ddd (15.5, 14.0, 6.0) b: 2.37, ddd (15.5, 4.8, 3.2)	a: 1.73, m b: 1.62, m
3				3.37, dd (11.5, 4.0)		3.30, dd (12.0, 4.0)
4	2.52, m	3.13, dd (6.5, 4.5)				
5	a: 2.87, dd (18.5,9.5) b: 2.19, dd (18.5,4.0)	4.46, dd (11.5, 4.5)	2.36, dd (14.0, 3.5)	1.88, m	1.67, m	1.05, m
6			a: 2.83, dd (17.5, 14.0) b: 2.75, dd (17.5, 3.5)	a: 2.79, dd (18.0, 13.5) b: 2.77, dd (18.0, 4.5)	a: 1.79, m b: 1.70, m	a: 1.79, m b: 1.52, m
7	5.56, m	4.88, br s			a: 2.17, m b: 1.68, m	a: 1.98, m b: 1.66, m
8	2.46, t (5.5)	2.06, m				
9					2.70, d (5.0)	1.95, m
10	3.28, m	3.65, m				
11	1.75, m	1.86, dd (10.5, 6.5)	7.49, d (8.5)	7.47, d (8.0)	5.44, d (5.0)	a: 2.27, dd (13.5, 5.5) b: 1.41, m
12	5.68, d (10.0)	5.73, d (10.5)	8.17, dd (8.5, 2.5)	8.14, dd (8.0, 2.0)		4.99, ddd (13.0, 5.5, 2.0)
13						
14	1.14, d (5.5)	0.89, d (6.5)	8.57, d (2.5)	8.55, d (2.0)	3.76, br s	3.77, s
15						
16	1.21, s	1.20, s				
17	1.33, s	1.33, s	2.64, s	2.63, s	2.09, s	1.97, d (2.0)
18	0.98. d (6.5)	1.16, d (6.5)	1.17, s	0.99, s	1.17, s	1.06, s
19	1.73, dd (2.5, 1.0)	1.83, br s	1.23, s	1.08, s	1.09, s	0.88, s
20	4.05, m	1.90, s	1.48, s	1.27, s	0.95, s	1.08, s
5-OH		5.92, d (11.5)				
9-OH	5.62, s	5.95, s				
	8.02, m	8.06, m				
12-OBz	7.59, m	7.61, m				
	7.47, m	7.49, m				
13-OAc	2.14, s	2.11, s				

Table 5. ^{13}C NMR data of compounds **14**–**17**, **19**, and **20** in $CDCl_3$ at 125 MHz (δ_C in ppm).

Position	14	15	16	17	19	20
1	159.7	154.6	36.8	35.9	38.1	38.7
2	136.7	144.3	34.6	27.5	34.2	27.3
3	208.7	207.5	214.0	78.0	215.0	78.6
4	44.4	56.3	47.6	39.1	48.1	39.0
5	29.8	71.1	49.2	48.3	54.1	53.6
6	142.3	138.0	36.5	36.1	21.7	20.8
7	126.6	125.5	197.4 [a]	198.5	33.9	34.8
8	42.3	40.2	130.8	130.8	61.0	61.0
9	78.0	78.7	158.2	159.9	50.1	49.2
10	54.3	48.0	38.3	38.5	40.9	39.2
11	42.8	43.5	125.2	124.8	102.9	24.0
12	77.8	75.7	133.4	133.2	148.1	75.6
13	65.5	65.4	135.9	135.5	144.7	155.6
14	36.0	38.5	128.3	128.1	54.5	56.2
15	26.0	25.1	197.3 [a]	197.4	126.2	128.9
16	23.9	24.3			170.5	174.1
17	17.1	16.7	26.9	26.8	9.0	8.9
18	15.3	11.9	25.2	27.6	25.9	29.1
19	10.3	10.6	21.7	15.2	22.4	16.1
20	67.6	27.2	22.8	23.3	15.0	19.3
12-OBz	166.4	166.4				
	133.4	133.4				
	130.1	130.1				
	129.9	129.9				
	128.7	128.7				
13-OAc	173.9	174.1				
	21.3	21.2				

[a]: Exchangeable.

2.1.13. 16-Nor-3β-hydroxy-abieta-8,11,13-trien-7,15-dione (**17**)

Compound **17** was obtained as a colorless crystal with a molecular formula of $C_{19}H_{24}O_3$ identified by HR-ESIMS *m/z* 301.1803 $[M + H]^+$ (calcd. for $C_{19}H_{25}O_3$ 301.1798). The inspection of 1D (Tables 4 and 5) and 2D NMR data revealed that **17** was a 16-nor-abieta-8,11,13-triene diterpenoid [45]. The ^1H and ^{13}C NMR data of **17** was close to those of **16**, except for a hydroxy group that was situated at C-3 (δ_C 78.0) by the confirmation of the ^1H–^1H COSY cross-peaks between H_2-1/H_2-2/H-3 as well as the HMBC correlations from H_2-1 to C-3 and H_3-18 to C-3. The H-3 [δ_H 3.37 (dd, J = 11.5, 4.0)] was identified as α-oriented by the NOESY correlations of H-3/H-5/H_3-18 and the comparison of the proton signals for **17** with those of the similar compound 3β-hydroxy-abieta-8,11,13-trien-7-one [46]. The structure of **17** was identified as 16-nor-3β-hydroxy-abieta-8,11,13-trien-7,15-dione.

2.1.14. ent-8β,14β-Epoxyabieta-3-one-11,13(15)-dien-16,12-olide (**19**)

Compound **19** was purified as a colorless gum. The molecular formula was calculated as $C_{20}H_{24}O_4$ by HR-ESIMS *m/z* 329.1753 $[M + H]^+$ (calcd. for $C_{20}H_{25}O_4$ 329.1747). The 1D (Tables 4 and 5) and 2D NMR data of **19** revealed four methyls [δ_H 2.09 (3H), δ_C 9.0, CH_3-17; δ_H 1.17 (3H), δ_C 25.9, CH_3-18; δ_H 1.09 (3H), δ_C 22.4, CH_3-19; δ_H 0.95 (3H), δ_C 15.0, CH_3-20], four methylenes [δ_H 2.05, 1.75, δ_C 38.1, CH_2-1; δ_H 2.65, 2.37, δ_C 34.2, CH_2-2; δ_H 1.79, 1.70, δ_C 21.7, CH_2-6; δ_H 2.17, 1.68, δ_C 33.9, CH_2-7], four methine (δ_H 1.67, δ_C 54.1, CH-5; δ_H 2.70, δ_C 50.1, CH-9; δ_H 5.44, δ_C 102.9, CH-11; δ_H 3.76, δ_C 54.5, CH-14), six quaternary carbons (δ_C 48.1, C-4; δ_C 61.0, C-8; δ_C 40.9, C-10; δ_C 148.1, C-12; δ_C 144.7, C-13; δ_C 126.2, C-15), and two carbonyl carbons (δ_C 215.0, C-3; δ_C 170.5, C-16). The structure of **19** was suggested an abietane-type diterpenoid with a ketone carbon at C-3, an epoxy ring fused at C-8 and C-14, a double bond at $\Delta_{11,12}$, and an α-methyl-α,β-unsaturated δ-lactone ring formed as D ring according to the analysis of the COSY cross-peaks of H_2-1/H_2-2, H_2-5/H_2-6/H_2-7, and H-9/H-11, as well as the HMBC correlations from H_2-1 to C-3, C-5, and C-10, H_2-2 to C-3 and C-10, H-5 to C-4, C-18, C-19, and C-20, H_2-7 to C-5 and C-8, H-9 to C-1, C-5, C-8, C-12, C-14, and C-20, H-11 to C-8, C-9, C-12, and C-13, H-14 to C-7, C-8, C-12, and C-13, H_3-17 to C-13, C-15, and C-16, H_3-18 and H_3-19 to C-3 and C-4,

together with H_3-20 to C-1, C-9, and C-10. Comparison of the ^{13}C NMR data with those of the related compounds jolkinolide A [47] and gelomulide C [48] further evidenced the presence of an *ent*-abietane skeleton with 8*β*,14*β*-epoxide in **19**. Thus, **19** was established as ent-8β,14β-epoxyabieta-3-one-11,13(15)-dien-16,12-olide.

2.1.15. ent-8β,14β-Epoxyabieta-3α-hydroxy-13(15)-en-16,12-olide (**20**)

Compound **20** was purified as a colorless gum. The molecular formula was calculated as $C_{20}H_{28}O_4$ by HR-ESIMS *m/z* 333.2067 $[M + H]^+$ (calcd. for $C_{20}H_{29}O_4$ 333.2060). The ^1H and ^{13}C NMR data (Tables 4 and 5) of **20** were close to those of **19** suggesting that the skeleton of **20** was an *ent*-abietane with 8*β*,14*β*-epoxide. Instead of the ketone carbon at C-3 in **19**, a hydroxyl group was connected to C-3 (δ_C 78.6) based on the inspection of the ^1H–^1H COSY cross-peaks between H_2-1/H_2-2/H-3 together with the HMBC correlations from H-3 to C-1, C-4, C-18, and C-19. Saturated methylene (δ_H 2.27, 1.41, δ_C 24.0) and an oxygenated methine (δ_H 4.99, δ_C 75.6) were assigned to be at C-11 and C-12, respectively, according to the analysis of the ^1H–^1H COSY cross-peaks between H-9/H_2-11/H-12 together with the HMBC correlations from H_2-11 to C-8, C-10, and C-13, as well as H-12 to C-13 and C-15. The structure was found to be highly similar to the NMR features of gelomulide A [48], except for instead of the hydroxyl group at C-3 in **20**. The configuration of 3-OH was deduced to be *α*-oriented as the proton signal of H-3 at 3.30 (dd, *J* = 12.0, 4.0 Hz) [49,50]. It was also supported by the NOESY correlations of H-3/H-5/H-9/H_3-18. The structure of **20** was established as ent-8β,14β-epoxyabieta-3α-hydroxy-13(15)-en-16,12-olide.

The known compounds were identified as isoterracinolide A (**10**) [36], isoterracinolide B (**11**) [36], 12-*O*-benzoyl-13-acetoxy-4,20-dideoxyphorbol-4-ene (**12**) [51,52], crotignoid K (**13**) [42], 16-*nor*-abieta-8,11,13-trien-3,15-dione (**18**) [53], helioscopinolide E (**21**) [54], helioscopinolide C (**22**) [54], helioscopinolide A (**23**) [54], *ent*-kauran-16*β*-ol-3-one (**24**) [55], cleomiscosin A (**25**) [56], (+)-syringaresinol (**26**) [57], dimeric coniferyl acetate (**27**) [58], vanillin (**28**) [59], 4-hydroxybenzaldehyde (**29**) [60], coniferol alcohol (**30**) [61], and indole-3-carboxaldehyde (**31**) [62] by comparison of the NMR data with those of the literature.

2.2. HIV-1 Latency Reversal Activity of Isolated Compounds in Vitro

Jurkat cells with a full-length integrated HIV-1 provirus that have been modified to contain a GFP coding region in place of the env gene (J-lat 10.6 cells) were used for HIV-1 anti-latency activity, cytotoxicity, and cellular activation testing. All 31 compounds were tested at 1, 10, and 100 μM. Through the GFP expression of J-lat 10.6 cells, it was determined that compounds **12**, **13**, **14**, **21**, **26**, and **27** showed HIV-1 latency reversal activity (Figure 4). These compounds were further tested at additional concentrations to determine dose response and toxicity curves (Figure 5A–F). Cell viability for all isolated compounds is presented in Figure S106 in the supplementary material.

4*β*-Crotignoid K (**14**) showed high reactivation levels into nM concentrations, ~250-fold less than crotignoid K (**13**), which is a stereoisomer of **14**, differing only in the configuration on C-4 (Figure 6). The striking difference between these compounds isolated from *E. usambarica* demonstrated a structure-activity relationship (SAR) of an important cellular trigger to induce HIV-1 proviral transcription. A similar SAR has recently been described between protein kinase C (PKC) agonists, 4-deoxyphorbol (4*β*-dPEA), phorbol myristate acetate (PMA), and prostratin [63].

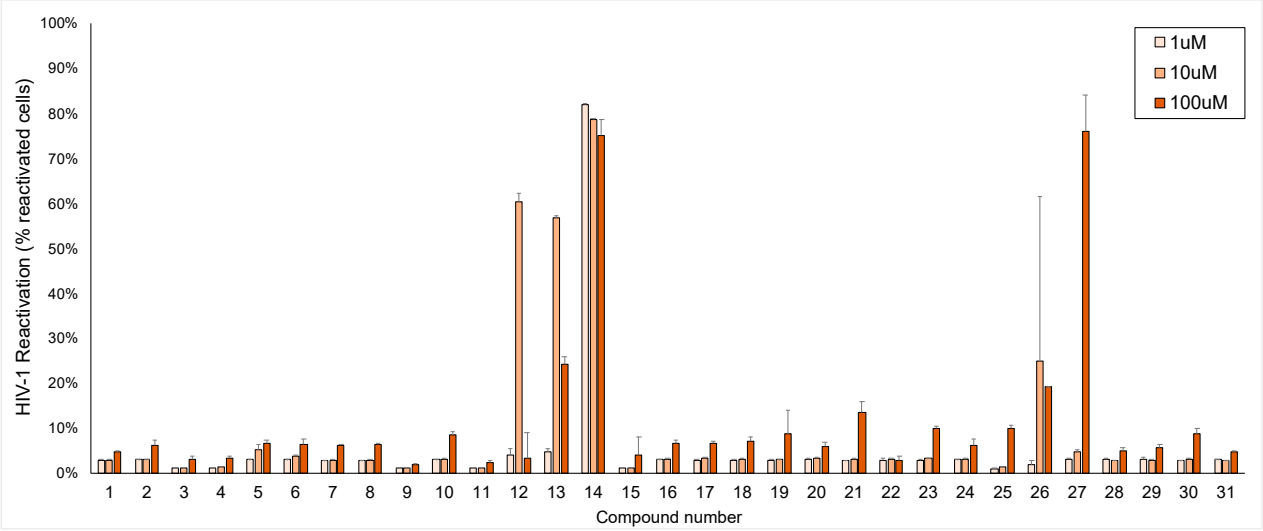

Figure 4. HIV-1 latency reversal activity of compounds **1**–**31** on J-Lat 10.6 cells in vitro.

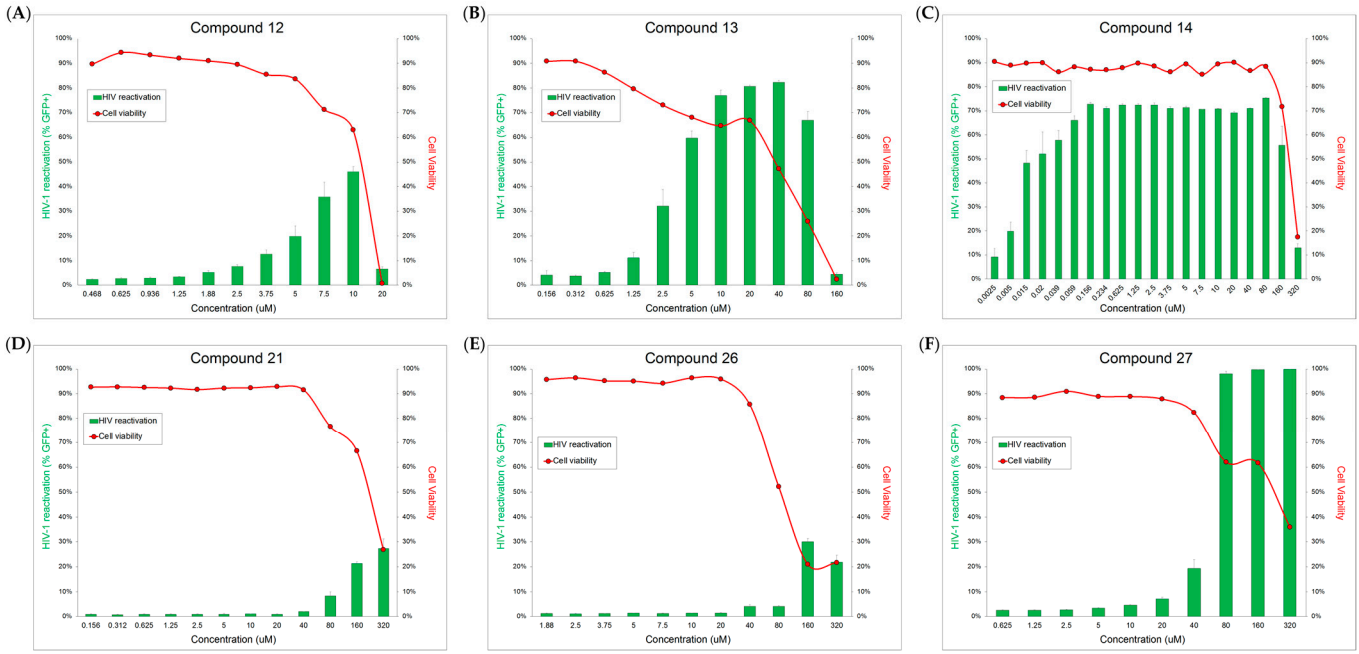

Figure 5. HIV-1 latency reversal activity dose-response (green bar) and cytotoxicity (red curve) of active compounds **12**–**14**, **21**, **26**, and **27** at additional concentrations. (**A**) dose-response experiments of **12** in a series concentration from 0.468 to 20 μM; (**B**) dose-response experiments of **13** in a series concentration from 0.158 to 160 μM; (**C**) dose-response experiments of **14** in a series concentration from 0.0025 to 320 μM; (**D**) dose-response experiments of **21** in a series concentration from 0.156 to 320 μM; (**E**) dose-response experiments of **26** in a series concentration from 1.88 to 320 μM; (**F**) dose-response experiments of **27** in a series concentration from 0.625 to 320 μM.

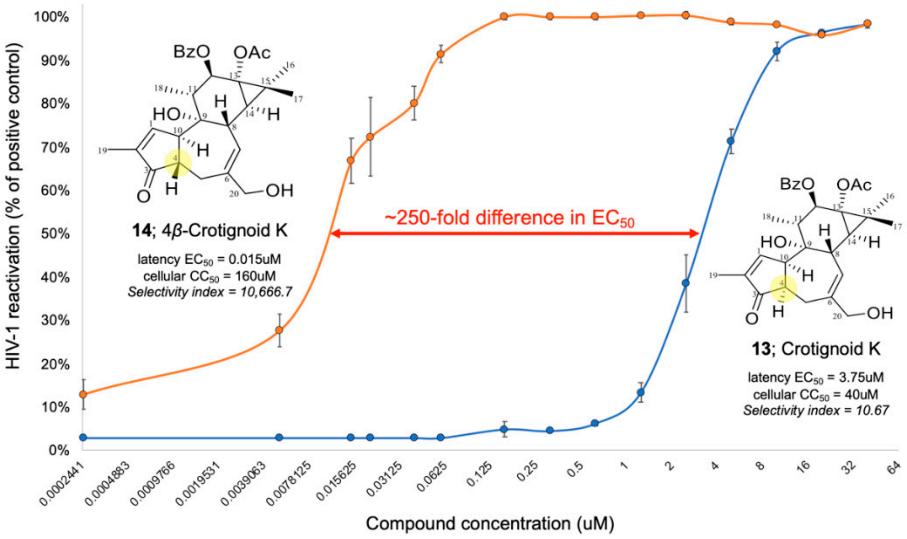

Figure 6. HIV-1 reactivation dose-response for stereoisomers crotignoid K (**13**) and 4*β*-crotignoid K (**14**).

Euphorbia species have been shown to be enriched for compounds capable of protein kinase C (PKC) activation in human cells [5,9,11,14,15]. In order to determine whether our active compounds were acting through PKC, we evaluated the latency reversal activity of each of these compounds in the presence and absence of a pan-PKC inhibitor, Gö6983 (Figure 7). Compounds **12**, **13**, **14**, and **21** all showed reduced efficacy, indicating likely activation of PKC as their primary mechanism of action. In contrast, compounds **26** and **27** did not show a significant reduction in their activity when PKC was inhibited. In addition, these compounds did not increase CD69 expression (a hallmark of PKC activation), further suggesting an alternative (non-PKC) mechanism of latency reversal.

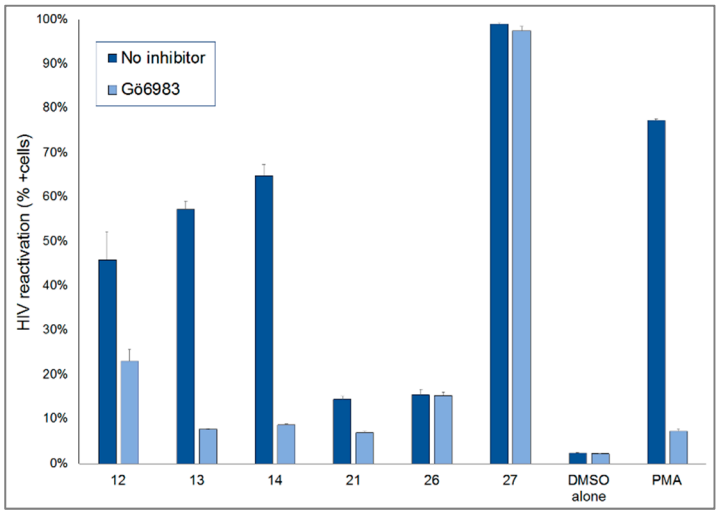

Figure 7. Effect of PKC inhibition on HIV-1 reactivation of compounds **13**–**14**, **21**, **26**, and **27**.

3. Discussion

In this study, 15 new diterpenoids, together with 16 known compounds, were isolated from the dichloromethane phase of methanolic extract of the medicinal plant *E. usambarica*. Compound **1** exhibited a 6/6/3-fused ring system with an *α*-methyl-*α*,*β*-unsaturated cyclopentanone moiety to construct a rare diterpenoid lactone, this skeleton was the second time discovered from nature [34]. The other compounds could be summarized in 4 types of

diterpenoids, including jatrophanes (**2**–**11**), tiglianes (**12**–**15**), abietanes (**16**–**23**), and kaurane (**24**), alone with coumarinolignoid (**25**), lignan (**26**), coniferyl acetate (**27**), and benzenoids (**28**–**31**). Especially, usambariphanes A (**2**) and B (**3**) displayed an unusual lactone ring constructed between C-17 and C-2 in the jatrophane structure, which is different from such lactone ring commonly constructed between C-17 and C-3 or between C-17 and C-5.

Furthermore, compounds **12**–**14**, **21**, **26**, and **27** showed significant HIV-1 latency reversal activity demonstrated by the GFP expression of J-lat 10.6 cells. 4β-Crotignoid K (**14**) showed the reactivation of HIV-1 latency at a very low concentration of EC_{50} about 0.015 μM and a higher CC_{50} concentration than 160 μM. The stereoisomer, crotignoid K (**13**), showed the EC_{50} and CC_{50} concentrations about 3.75 and 40 μM, respectively, indicating that 4β-crotignoid K (**14**) was provided with higher safety and efficacy. There is a 250-fold difference in EC_{50} and ~1000-fold difference in selectivity index (CC_{50}/EC_{50}) between these compounds. The structural difference between **13** and **14** is only in the relative configuration on C-4. However, they demonstrated dramatically different biological activity, indicating that the configuration on C-4 of tigliane-type diterpenoids is critical to HIV-1 latency reversal activity and likely reflects improved PKC activation. The primary mechanism of the active compounds **12**–**14** and **21** for the HIV-1 latency reversal activity was activation of PKC.

Currently, LRAs are still under investigation and have not been approved by the US Food and Drug Administration (US-FDA). Therefore, the intensive study of LRAs is an important topic, especially to discover new candidates from natural sources. For example, a known LRA, ingenol, is isolated originally from *Euphorbia peplus* [64] and is a US-FDA-approved topical treatment for actinic keratosis (AK) [65], showed a significant effect in the reactivation of HIV-1 latency through the PKC pathway [65]. Both compound **14** and ingenol mebutate are *Euphorbia* diterpenoids and the potent PKC agonists. In addition, compound **14** presented the lower cytotoxicity, indicating **14** is a promising candidate for the development of an LRA.

In contrast, (+)-syringaresinol (**26**) and dimeric coniferyl acetate (**27**) did not increase CD69 expression, further suggesting a non-PKC mechanism of latency reversal that merits further exploration.

4. Materials and Methods

4.1. General Experimental Procedures

Optical rotation was performed on a Perkin-Elmer 341 polarimeter. 1D and 2D NMR spectra were recorded on a Bruker Avance DRX 500 spectrometer at 500 MHz (^{1}H) and 125 MHz (^{13}C). Chemical shifts were reported in parts per million (δ), and the coupling constants (J) were expressed in Hertz. The residual peaks of the deuterated solvents were taken as reference points. The NMR data were acquired and processed with MestReNova v12.0.0−20080 software. High-resolution MS spectra were acquired on an FTHRMS-Orbitrap (Thermo-Finnigan) mass spectrometer equipped with an ESI ion source in positive ionization mode. HPLC analyses were performed with a Shimadzu LC-10AS pump interface equipped with a Shimadzu SPD-10A UV–VIS detector (Shimadzu Inc., Kyoto, Japan) using Kinetex C18 column (5 μm, 100 Å, 250 × 4.6 mm), Kinetex Biphenyl column (5 μm, 100 Å, 250 × 4.6 mm), Kinetex XB-C18 column (5 μm, 100 Å, 250 × 10 mm), and/or Luna® Phenyl-Hexyl column (5 μm, 250 × 10 mm) (Phenomenex Inc., Torrance, CA, USA) using a mixture of acetonitrile–H_2O or mixture of methanol–H_2O as mobile phase. Rotational planar chromatography (RPC) was performed on self-coated silica plates (Kieselgel 60 GF_{254}, 15 μm, Merck, Germany) using a Chromatotron apparatus (Harrison Research, Palo Alto, CA, USA). Silica gel (Kieselgel 60, 63–200 μm, Merck, Darmstadt, Germany), polyamide (MP Polyamide, 50−160 μm, MP Biomedicals, Irvine, CA, USA), and Sephadex LH-20 gel (Pharmacia Fine Chemicals AB, Uppsala, Sweden) were used for column chromatography (CC). Thin-layer chromatography (TLC) was carried out using silica gel (Kieselgel 60 F_{254}, Merck) and RP-C18 (F_{254s}, Merck) pre-coated plates, and the preparative TLC (pre-TLC) was performed on glass sheet silica gel pre-coated plates

(20 × 20 cm, Kieselgel 60 F_{254}, Merck). The compounds were detected with a developer (20% H_2SO_4 (*v*/*v*) with 5% vanillin (*w*/*v*) in ethanol) followed by heating (120 °C).

4.2. Plant Material

Euphorbia usambarica Pax. (Euphorbiaceae) was collected in Taita Taveta county, Kenya in 2019. Identification was performed by Peter Waweru Mwangi (Department of Medical Physiology, School of Medicine, University of Nairobi, Nairobi, Kenya). A voucher specimen (No. EU-001) has been deposited in the Herbarium of the Department of Pharmacognosy, University of Szeged, Szeged, Hungary.

4.3. Extraction and Isolation

The dried stem and root part (2.7 kg) were chopped and extracted with methanol (MeOH, 15 L) at room temperature. After removing the solvent, the crude methanolic extract (EU, 220.0 g) was dissolved in 50% $MeOH_{aq}$ and subjected to liquid–liquid partition to afford *n*-hexane (EU-H), dichloromethane (CH_2Cl_2, EU-C), ethyl acetate (EtOAc, EU-E), and water-soluble residue (EU-W) phases. The EU-C (25.7 g) was subjected to polyamide CC with MeOH–H_2O mixture solvent system (40%, 60%, 80%, and 100% $MeOH_{aq}$; EU-C-P1–P4). The EU-C-P1 (8.7 g) was further subjected to normal phase CC (silica gel, 63–200 μm) with a gradient solvent system of *n*-hexane–EtOAc–MeOH mixtures (from 40:5:1 to 0:8:1) to obtain ten subfractions (EU-C-P1-1–10) based on the TLC monitoring. EU-C-P1-2 (29.7 mg) was subjected to Sephadex LH-20 CC with the eluent of CH_2Cl_2–EtOAc–MeOH (1:1:6) to yield 6 subfractions (EU-C-P1-2/1–6), and EU-C-P1-2/2 was further separated by RP-HPLC on Kinetex XB-C18 column with an isocratic solvent system of MeCN–H_2O (60:40, 2.0 mL/min) to yield compound **18** (1.1 mg). EU-C-P1-3 (895.5 mg) was separated by Sephadex LH-20 CC using CH_2Cl_2–EtOAc–MeOH (1:1:6) as eluent to obtain 5 subfractions (EU-C-P1-3/1–5). EU-C-P1-3/2 (245.5 mg) was further subjected to RPC (thickness 2 mm) using a gradient system of CH_2Cl_2–MeOH (from 100:0 to 15:1) to obtain 5 subfractions (EU-C-P1-3/2/1–5). Compound **21** (63.5 mg) was purified by recrystallization (MeOH) from EU-C-P1-3/2/1 (133.8 mg), and the residue of this fraction was further purified by RP-HPLC on Kinetex XB-C18 column with an isocratic system of MeCN–H_2O (53:47, 2.0 mL/min) to yield compounds **16** (4.0 mg) and **19** (3.5 mg). EU-C-P1-3/2/2 (38.6 mg) was subjected to prep-TLC using CH_2Cl_2–MeOH (60:1) as the eluent to obtain 5 subfractions (EU-C-P1-3/2/2/1–5), then the second and third subfractions were purified by RP-HPLC on Kinetex XB-C18 column with an isocratic system of MeCN–H_2O (65:35, 2.0 mL/min) to yield compounds **10** (4.7 mg) and **15** (1.0 mg), respectively. EU-C-P1-3/3 (178.5 mg) was subjected to RPC (thickness 2 mm) using a gradient system of *n*-hexane–CH_2Cl_2–MeOH (from 5:1:0 to 20:1) to obtain 9 subfractions (EU-C-P1-3/3/1–9), then the second subfraction (23.0 mg) was purified by RP-HPLC on Kinetex Biphenyl column with an isocratic system of MeOH–H_2O (75:25, 1.0 mL/min) to yield compound **24** (2.7 mg). EU-C-P1-3/4 (39.3 mg) was separated by prep-TLC using CH_2Cl_2–MeOH (60:1) as eluent to yield compound **28** (11.0 mg). EU-C-P1-3/5 (10.2 mg) was purified by prep-TLC using CH_2Cl_2–MeOH (35:1) as eluent to yield compound **29** (1.8 mg). EU-C-P1-4 (1060.4 mg) was subjected to Sephadex LH-20 gel chromatography eluting with CH_2Cl_2–EtOAc–MeOH (1:1:6) to obtain 9 subfractions (EU-C-P1-4/1–9). EU-C-P1-4/2 (442.8 mg) was further separated by RPC (thickness 2 mm) using a gradient system of *n*-hexane–CH_2Cl_2–MeOH (from 1:1:0 to 10:1) to obtain 8 subfractions (EU-C-P1-4/2/1–9). EU-C-P1-4/2/2 (14.1 mg) was further purified by RP-HPLC on Kinetex XB-C18 column with an isocratic solvent system of MeCN–H_2O (50:50, 2.0 mL/min) to yield compound **27** (4.6 mg). EU-C-P1-4/2/4 (68.6 mg) was further purified by RP-HPLC on Kinetex XB-C18 column with isocratic solvent system of MeCN–H_2O (55:45, 2.0 mL/min) to yield compounds **1** (1.1 mg), **2** (4.0 mg), **3** (1.5 mg), **4** (2.0 mg), **5** (5.2 mg), **6** (2.5 mg), **7** (3.2 mg), **8** (1.4 mg), **9** (1.7 mg), **11** (3.7 mg), and **22** (2.2 mg). EU-C-P1-4/2/6 (60.4 mg) was purified by RP-HPLC on Kinetex XB-C18 column with an isocratic solvent system of MeCN–H_2O (50:50, 2.0 mL/min) to yield compounds **12** (2.3 mg) and **13** (4.2 mg). EU-C-P1-4/2/7 (40.9 mg) was purified by RP-HPLC on

Luna® Phenyl-Hexyl column with an isocratic system of MeCN–H_2O (51:49, 2.0 mL/min) to yield compound **14** (1.4 mg). EU-C-P1-4/4 (218.3 mg) was further separated by RPC (thickness 2 mm) using a gradient system of CH_2Cl_2–MeOH (from 100:0 to 20:1) to obtain 6 subfractions (EU-C-P1-4/4/1–6). EU-C-P1-4/4/2 (52.4 mg) was further chromatographed by Sephadex LH-20 CC eluting with CH_2Cl_2–EtOAc–MeOH (1:1:6) to obtain 3 subfractions, then the second subfraction was purified by RP-HPLC on Kinetex XB-C18 column with an isocratic solvent system of MeCN–H_2O (53:47, 2.0 mL/min) to yield compounds **17** (2.8 mg), **20** (2.7 mg), and **23** (14.2 mg). EU-C-P1-4/8 (11.6 mg) was purified by RP-HPLC on Kinetex XB-C18 column with an isocratic solvent system of MeCN–H_2O (35:65, 2.0 mL/min) to yield compounds **30** (1.3 mg) and **31** (1.6 mg). EU-C-P1-7 (480.1 mg) was subjected to Sephadex LH-20 CC eluting with CH_2Cl_2–EtOAc–MeOH (1:1:6) to obtain 8 subfractions (EU-C-P1-7/1–8). EU-C-P1-7/6 was further purified by RP-HPLC on Kinetex XB-C18 column with an isocratic system of MeOH–H_2O (48:52, 2.0 mL/min) to yield compound **26** (2.6 mg). Compound **25** (8.3 mg) was yielded by re-crystallization (MeOH) from EU-C-P1-7/7.

4.4. Physical Characteristic of New Compounds

*Euphordraculoate C (**1**)*: Colorless gum; $[\alpha]_D^{28}$ −63 (*c* 0.05, $CHCl_3$); the ^1H and ^{13}C NMR spectroscopic data, see Tables 1 and 2; HR-ESIMS *m/z* 493.2237 $[M + H]^+$ (calcd. for $C_{29}H_{33}O_7$ 493.2221), *m/z* 515.2046 $[M + Na]^+$ (calcd. for $C_{29}H_{32}O_7Na$ 515.2040).

*Usambaricinophane A (**2**)*: White amorphous powder; $[\alpha]_D^{28}$ −17 (*c* 0.20, $CHCl_3$); the ^1H and ^{13}C NMR spectroscopic data, see Tables 1 and 2; HR-ESIMS *m/z* 789.3327 $[M + H]^+$ (calcd. for $C_{40}H_{53}O_{16}$ 789.3328), *m/z* 811.3169 $[M + Na]^+$ (calcd. for $C_{40}H_{52}O_{16}Na$ 811.3148).

*Usambaricinophane B (**3**)*: White amorphous powder; $[\alpha]_D^{28}$ −7 (*c* 0.07, $CHCl_3$); the ^1H and ^{13}C NMR spectroscopic data, see Tables 1 and 2; HR-ESIMS *m/z* 803.3488 $[M + H]^+$ (calcd. for $C_{41}H_{55}O_{16}$ 803.3485), *m/z* 825.3333 $[M + Na]^+$ (calcd. for $C_{41}H_{54}O_{16}Na$ 825.3304).

*Usambaricinophane C (**4**)*: colorless crystal; $[\alpha]_D^{28}$ +34 (*c* 0.10, $CHCl_3$); the ^1H and ^{13}C NMR spectroscopic data, see Tables 1 and 2; HR-ESIMS *m/z* 789.3346 $[M + H]^+$ (calcd. for $C_{40}H_{53}O_{16}$ 789.3328) *m/z* 811.3171 $[M + Na]^+$ (calcd. for $C_{40}H_{52}O_{16}Na$ 811.3148).

*Usambaricinophane D (**5**)*: Colorless crystal; $[\alpha]_D^{28}$ +54 (*c* 0.30, $CHCl_3$); the ^1H and ^{13}C NMR spectroscopic data, see Tables 1 and 2; HR-ESIMS *m/z* 787.3193 $[M + H]^+$ (calcd. for $C_{40}H_{51}O_{16}$ 787.3172), *m/z* 809.3011 $[M + Na]^+$ (calcd. for $C_{40}H_{50}O_{16}Na$ 809.2991).

*Usambaricinophane E (**6**)*: Colorless crystal; $[\alpha]_D^{28}$ +54 (*c* 0.15, $CHCl_3$); the ^1H and ^{13}C NMR spectroscopic data, see Tables 1 and 2; HR-ESIMS *m/z* 801.3356 $[M + H]^+$ (calcd. for $C_{41}H_{53}O_{16}$ 801.3328) *m/z* 823.3170 $[M + Na]^+$ (calcd. for $C_{41}H_{52}O_{16}Na$ 823.3148).

*Usambaricinophane F (**7**)*: Colorless crystal; $[\alpha]_D^{28}$ +15 (*c* 0.20, $CHCl_3$); the ^1H and ^{13}C NMR spectroscopic data, see Table 3; HR-ESIMS *m/z* 761.3383 $[M + H]^+$ (calcd. for $C_{39}H_{53}O_{15}$ 761.3379), *m/z* 783.3215 $[M + Na]^+$ (calcd. for $C_{39}H_{52}O_{15}Na$ 783.3198).

*Usambaricinophane G (**8**)*: Colorless crystal; $[\alpha]_D^{28}$ +15 (*c* 0.08, $CHCl_3$); the ^1H and ^{13}C NMR spectroscopic data, see Table 3; HR-ESIMS *m/z* 764.3230 $[M + H]^+$ (calcd. for $C_{41}H_{50}O_{13}N$ 764.3277), *m/z* 786.3098 $[M + Na]^+$ (calcd. for $C_{41}H_{49}O_{13}NNa$ 786.3096).

*Isoterracinolide C (**9**)*: White amorphous powder; $[\alpha]_D^{28}$ -2 (*c* 0.10, $CHCl_3$); the ^1H and ^{13}C NMR spectroscopic data, see Table 3; HR-ESIMS *m/z* 775.31721 $[M + H]^+$ (calcd. for $C_{39}H_{51}O_{16}$ 775.3172), *m/z* 797.3011 $[M + Na]^+$ (calcd. for $C_{39}H_{50}O_{16}Na$ 797.2991).

*4β-Crotignoid K (**14**)*: White amorphous powder; $[\alpha]_D^{28}$ +48 (*c* 0.05, $CHCl_3$); the ^1H and ^{13}C NMR spectroscopic data, see Tables 4 and 5; HR-ESIMS *m/z* 495.2385 $[M + H]^+$ (calcd. for $C_{29}H_{35}O_7$ 495.2377), *m/z* 517.2202 $[M + Na]^+$ (calcd. for $C_{29}H_{34}O_7Na$ 517.2197).

*Euphodendriane B (**15**)*: White amorphous powder; $[\alpha]_D^{28}$ +12 (*c* 0.033, $CHCl_3$); the ^1H and ^{13}C NMR spectroscopic data, see Tables 4 and 5; HR-ESIMS *m/z* 495.2396 $[M + H]^+$ (calcd. for $C_{29}H_{35}O_7$ 495.2377), *m/z* 517.2209 $[M + Na]^+$ (calcd. for $C_{29}H_{34}O_7Na$ 517.2197).

*16-Nor-abieta-8,11,13-trien-3,7,15-trione (**16**)*: Colorless crystal; $[\alpha]_D^{28}$ +15 (*c* 0.20, $CHCl_3$); the ^1H and ^{13}C NMR spectroscopic data, see Tables 4 and 5; HR-ESIMS *m/z* 299.1648 $[M + H]^+$ (calcd. for $C_{19}H_{22}O_3$ 299.1642), *m/z* 321.1466 $[M + Na]^+$ (calcd. for $C_{19}H_{22}O_3Na$ 321.1461).

*16-Nor-3β-hydroxy-abieta-8,11,13-trien-7,15-dione (**17**)*: Colorless crystal; $[\alpha]_D^{28}$ −9 (*c* 0.20, $CHCl_3$); the ^1H and ^{13}C NMR spectroscopic data, see Tables 4 and 5; HR-ESIMS *m/z*

301.1803 $[M + H]^+$ (calcd. for $C_{19}H_{25}O_3$ 301.1798), *m/z* 323.1623 $[M + Na]^+$ (calcd. for $C_{19}H_{24}O_3Na$ 323.1618).

ent-8β,14β-Epoxyabieta-3-one-11,13(15)-dien-16,12-olide (***19***): Colorless gum; $[\alpha]_D^{28}$ +90 (*c* 0.20, $CHCl_3$); the ^1H and ^{13}C NMR spectroscopic data, see Tables 4 and 5; HR-ESIMS *m/z* 329.1753 $[M + H]^+$ (calcd. for $C_{20}H_{25}O_4$ 329.1747), *m/z* 351.1572 $[M + Na]^+$ (calcd. for $C_{20}H_{24}O_4Na$ 351.1567).

ent-8β,14β-Epoxyabieta-3α-hydroxy-13(15)-en-16,12-olide (***20***): Colorless gum; $[\alpha]_D^{28}$ +57 (*c* 0.20, $CHCl_3$); the ^1H and ^{13}C NMR spectroscopic data, see Tables 4 and 5; HR-ESIMS *m/z* 333.2067 $[M + H]^+$ (calcd. for $C_{20}H_{29}O_4$ 333.2060), *m/z* 355.1886 $[M + Na]^+$ (calcd. for $C_{20}H_{28}O_4Na$ 355.1880).

4.5. Cell Isolation and Culture

The HIV-1-infected Jurkat T cell line (J-Lat 10.6) was obtained in January 2019 from the NIH/ATCC HIV-1 Reagent Program (www.hivreagentprogram.org) and cultured in RPMI-based media supplemented with 10% fetal calf serum, 1% penicillin, and 1% streptomycin.

4.6. Flow Cytometry

After in vitro culture, J-lat cells were washed with phosphate-buffered saline (1× PBS) prior to staining with 0.1 µL fixable viability dye Live/Dead Aqua (Cat L34957, www.thermofisher.com) per 10^5 cells for 30 min at 4 °C. Simultaneously, J-lat cells were also stained with antibodies against CD69 conjugated to an APC fluorophore (APC anti-human CD69 antibody, biolegend.com). Cells were then washed and re-suspended in 1× PBS prior to flow cytometry acquisition evaluating for cellular viability, green fluorescent protein (GFP) expression, and CD69 expression. Flow cytometry was performed with a BD FACSCelesta or FACSCanoto flow cytometer with FACSDiva acquisition software (Becton Dickinson, Mountain View, CA) prior to analysis with FlowJo (TreeStar Inc., Ashland, OR, USA).

4.7. Compound Screening

Isolated compounds were resuspended in dimethyl sulfoxide (DMSO; Sigma-Aldrich, Burlington, USA), at a concentration of 10 mM, and diluted with PBS, and tested with J-lat 10.6 cells at concentrations of 100, 10, and 1 µM. J-lat 10.6 cells were tested with compounds at a concentration of 2.5×10^5 cells/mL. We performed a minimum of three replicates of each condition for all experiments. Negative controls contained 1% DMSO to account for any effect of DMSO in the highest dilution of compounds. Additional dilutions were tested for those compounds that showed reactivation through increased GFP production in J-lat 10.6 cells.

4.8. Statistical Analysis

Statistical significance was analyzed using software from GraphPad Prism Version 7.0c (GraphPad Software, San Diego, CA, USA). The mean values and standard deviations for all replicate J-lat results were calculated and used to create Figures 4–7. Where applicable, Students t-test was used to determine statistical significance of experimental mean results relative to negative controls.

5. Conclusions

In this study, 4*β*-crotignoid K (**14**) revealed a very higher effect improvement compared to crotignoid K (**13**), indicating that configuration at the C-4 of tigliane diterpenoids is critical to HIV-1 latency reversal activity. (+)-Syringaresinol (**26**) and dimeric coniferyl acetate (**27**) showed no exhibition of CD69 expression, suggesting a non-PKC mechanism of latency reversal. Our results provide insights into the stereochemistry importance of bioactive diterpenoids and suggest that isolated compounds from *E. usambarica* can further research and development into therapeutic strategies for HIV-1 management, particularly as reactivators of latent HIV-1.

Supplementary Materials: The following are available online at https://www.mdpi.com/article/10.3390/ph14070653/s1, Figures S1–S105: 1D-NMR, 2D-NMR, and HR-ESIMS spectra of compounds **1**–**9**, **14**–**16**, **19**, and **20**. Figure S106: 24 h cell viability after exposure to the compounds **1**–**31**.

Author Contributions: Conceptualization, Y.-C.T., A.M.S., and J.H.; methodology, A.M.S., and J.H.; software, Y.-C.T., N.K., R.A.N., J.E.B., and A.M.S.; validation, Y.-C.T., A.M.S., and J.H.; formal analysis, Y.-C.T., N.K., R.A.N., J.E.B., A.M.S., and J.H.; investigation, Y.-C.T., N.K., R.A.N., J.E.B., R.B., D.R., A.V., A.M.S., and J.H.; resources, P.W.M. and J.H.; data curation, Y.-C.T., and A.M.S.; writing—original draft preparation, Y.-C.T.; writing—review and editing, A.M.S. and J.H.; visualization, Y.-C.T., R.A.N., J.E.B., and A.M.S.; supervision, A.M.S. and J.H.; project administration, J.H.; funding acquisition, J.H. All authors have read and agreed to the published version of the manuscript.

Funding: This research was funded by the Economic Development and Innovation Operative Programme (GINOP-2.3.2-15-2016-00012) and the Ministry of Human Capacities, Hungary Grant (TUDFO/47138-1/2019-ITM FIKP). This work was supported by the National Research, Development and Innovation Fund (NKFI) under grant numbers K135845 and by ÚNKP-20-4 grant for co-author N. Kúsz.

Institutional Review Board Statement: The study was conducted according to the guidelines of the Declaration of Helsinki, and approved in 21 March 2021 by the Institutional Review Board of the University of Utah (IRB_0067637).

Informed Consent Statement: Informed consent was obtained from all subjects involved in the study.

Data Availability Statement: Data sharing not applicable.

Acknowledgments: T The following reagent was obtained through the NIH HIV Reagent Program, Division of AIDS, NIAID, NIH: J-Lat Full-Length Cells (10.6), ARP-9849, contributed by Eric Verdin. The authors appreciate the editorial assistance and comments by the editor and reviewers.

Conflicts of Interest: The authors declare no conflict of interest.

References

1. Spivak, A.M.; Planelles, V. HIV-1 eradication: Early trials (and tribulations). *Trends Mol. Med.* **2016**, *22*, 10–27. [CrossRef] [PubMed]
2. Andersen, R.J.; Ntie-Kang, F.; Tietjen, I. Natural product-derived compounds in HIV suppression, remission, and eradication strategies. *Antivir. Res.* **2018**, *158*, 63–77. [CrossRef] [PubMed]
3. Cary, D.C.; Peterlin, B.M. Natural products and HIV/AIDS. *AIDS Res. Hum. Retrovir.* **2018**, *34*, 31–38. [CrossRef] [PubMed]
4. Salehi, B.; Kumar, N.V.A.; Sener, B.; Sharifi-Rad, M.; Kilic, M.; Mahady, G.B.; Vlaisavljevic, S.; Iriti, M.; Kobarfard, F.; Setzer, W.N.; et al. Medicinal plants used in the treatment of human immunodeficiency virus. *Int. J. Mol. Sci.* **2018**, *19*, 1459. [CrossRef] [PubMed]
5. Mwine, J.T.; Van Damme, P. Why do Euphorbiaceae tick as medicinal plants? A review of Euphorbiaceae family and its medicinal features. *J. Med. Plants Res.* **2011**, *5*, 652–662.
6. Shi, Q.W.; Su, X.H.; Kiyota, H. Chemical and pharmacological research of the plants in genus *Euphorbia*. *Chem. Rev.* **2008**, *108*, 4295–4327. [CrossRef]
7. Vasas, A.; Hohmann, J. *Euphorbia* diterpenes: Isolation, structure, biological activity, and synthesis (2008–2012). *Chem. Rev.* **2014**, *114*, 8579–8612. [CrossRef]
8. Patil, S.B.; Naikwade, N.S.; Magdum, C.S. Review on phytochemistry and pharmacological aspects of *Euphorbia hirta* Linn. *Asian J. Pharm. Res. Health Care* **2009**, *1*, 113–133.
9. Kumar, S.; Malhotra, R.; Kumar, D. *Euphorbia hirta*: Its chemistry, traditional and medicinal uses, and pharmacological activities. *Pharmacogn. Rev.* **2010**, *4*, 58–61. [CrossRef] [PubMed]
10. Özbilgin, S.; Saltan Çitoğlu, G. Uses of some *Euphorbia* species in traditional medicine in turkey and their biological activities. *Turk. J. Pharm. Sci.* **2012**, *9*, 241–255.
11. Lee, J.W.; Jin, Q.; Jang, H.; Lee, D.; Han, S.B.; Kim, Y.; Hong, J.T.; Lee, M.K.; Hwang, B.Y. Jatrophane and ingenane-type diterpenoids from *Euphorbia kansui* inhibit the LPS-induced NO production in RAW 264.7 cells. *Bioorg. Med. Chem. Lett.* **2016**, *26*, 3351–3354. [CrossRef] [PubMed]
12. Redei, D.; Forgo, P.; Molnar, J.; Szabo, P.; Zorig, T.; Hohmann, J. Jatrophane diterpenoids with multidrug resistance-modulating activity from *Euphorbia mongolica* Prokh. *Tetrahedron* **2012**, *68*, 8403–8407. [CrossRef]
13. Corea, G.; Di Pietro, A.; Dumontet, C.; Fattorusso, E.; Lanzotti, V. Jatrophane diterpenes from *Euphorbia* spp. as modulators of multidrug resistance in cancer therapy. *Phytochem. Rev.* **2009**, *8*, 431–447. [CrossRef]

14. Nothias-Scaglia, L.F.; Retailleau, P.; Paolini, J.; Pannecouque, C.; Neyts, J.; Dumontet, V.; Roussi, F.; Leyssen, P.; Costa, J.; Litaudon, M. Jatrophane diterpenes as inhibitors of chikungunya virus replication: Structure-activity relationship and discovery of a potent lead. *J. Nat. Prod.* **2014**, *77*, 1505–1512. [CrossRef] [PubMed]
15. Remy, S.; Litaudon, M. Macrocyclic diterpenoids from Euphorbiaceae as a source of potent and selective inhibitors of chikungunya virus replication. *Molecules* **2019**, *24*, 2336. [CrossRef]
16. Islam, M.T. Diterpenes and their derivatives as potential anticancer agents. *Phytother. Res.* **2017**, *31*, 691–712. [CrossRef] [PubMed]
17. Fattahian, M.; Ghanadian, M.; Ali, Z.; Khan, I.A. Jatrophane and rearranged jatrophane-type diterpenes: Biogenesis, structure, isolation, biological activity and SARs (1984–2019). *Phytochem. Rev.* **2020**, *19*, 265–336. [CrossRef]
18. Kusz, N.; Orvos, P.; Bereczki, L.; Fertey, P.; Bombicz, P.; Csorba, A.; Talosi, L.; Jakab, G.; Hohmann, J.; Redei, D. Diterpenoids from *Euphorbia dulcis* with potassium ion channel inhibitory activity with selective G protein-activated inwardly rectifying ion channel (GIRK) blocking effect. *J. Nat. Prod.* **2018**, *81*, 2483–2492. [CrossRef]
19. Rawal, M.K.; Shokoohinia, Y.; Chianese, G.; Zolfaghari, B.; Appendino, G.; Taglialatela-Scafati, O.; Prasad, R.; Di Pietro, A. Jatrophanes from *Euphorbia squamosa* as potent inhibitors of *Candida albican*s multidrug transporters. *J. Nat. Prod.* **2014**, *77*, 2700–2706. [CrossRef] [PubMed]
20. Tsai, J.Y.; Redei, D.; Forgo, P.; Li, Y.; Vasas, A.; Hohmann, J.; Wu, C.C. Isolation of phorbol esters from *Euphorbia grandicornis* and evaluation of protein kinase c and human platelet-activating effects of *Euphorbiaceae. Diterpenes*. *J. Nat. Prod.* **2016**, *79*, 2658–2666. [CrossRef]
21. Park, K.H.; Koh, D.; Lee, S.; Jung, I.; Kim, K.H.; Lee, C.H.; Kim, K.H.; Lim, Y. Anti-allergic and anti-asthmatic activity of helioscopinin-A, a polyphenol compound, isolated from *Euphorbia helioscopia*. *J. Microbiol. Biotechnol.* **2001**, *11*, 138–142.
22. Islam, N.U.; Khan, I.; Rauf, A.; Muhammad, N.; Shahid, M.; Shah, M.R. Antinociceptive, muscle relaxant and sedative activities of gold nanoparticles generated by methanolic extract of *Euphorbia milii*. *BMC Complementary Altern. Med.* **2015**, *15*, 160. [CrossRef] [PubMed]
23. Spivak, A.M.; Planelles, V. Novel latency reversal agents for HIV-1 cure. *Annu. Rev. Med.* **2018**, *69*, 421–436. [CrossRef] [PubMed]
24. Wonderlich, E.R.; Subramanian, K.; Cox, B.; Wiegand, A.; Lackman-Smith, C.; Bale, M.J.; Stone, M.; Hoh, R.; Kearney, M.F.; Maldarelli, F.; et al. Effector memory differentiation increases detection of replication-competent HIV-l in resting CD4+ T cells from virally suppressed individuals. *PLoS Pathog.* **2019**, *15*, e1008074. [CrossRef] [PubMed]
25. Cary, D.C.; Fujinaga, K.; Peterlin, B.M. *Euphorbia kansui* reactivates latent HIV. *PLoS ONE* **2016**, *11*, e0168027. [CrossRef] [PubMed]
26. Pisano, M.B.; Cosentino, S.; Viale, S.; Spano, D.; Corona, A.; Esposito, F.; Tramontano, E.; Montoro, P.; Tuberoso, C.I.; Medda, R.; et al. Biological activities of aerial parts extracts of *Euphorbia characias*. *Biomed. Res. Int.* **2016**, *2016*, 1538703. [CrossRef] [PubMed]
27. Rasmussen, T.A.; Tolstrup, M.; Sogaard, O.S. Reversal of latency as part of a cure for HIV-1. *Trends Microbiol.* **2016**, *24*, 90–97. [CrossRef] [PubMed]
28. Liu, Q.; Li, W.; Huang, L.; Asada, Y.; Morris-Natschke, S.L.; Chen, C.H.; Lee, K.H.; Koike, K. Identification, structural modification, and dichotomous effects on human immunodeficiency virus type 1 (HIV-1) replication of ingenane esters from *Euphorbia kansui*. *Eur. J. Med. Chem.* **2018**, *156*, 618–627. [CrossRef] [PubMed]
29. Yan, S.L.; Li, Y.H.; Chen, X.Q.; Liu, D.; Chen, C.H.; Li, R.T. Diterpenes from the stem bark of *Euphorbia neriifolia* and their in vitro anti-HIV activity. *Phytochemistry* **2018**, *145*, 40–47. [CrossRef]
30. Valadão, A.L.C.; Pezzuto, P.; Silva, V.A.O.; Gonçalves, B.S.; Rossi, Á.D.; Cunha, R.D.; Siani, A.C.; Tostes, J.B.F.; Trovó, M.; Damasco, P.; et al. Reactivation of latent HIV-1 in vitro using an ethanolic extract from *Euphorbia umbellata* (Euphorbiaceae) latex. *PLoS ONE* **2018**, *13*, e0207664. [CrossRef]
31. Thiselton-Dyer W.T. *Euphorbia usambarica* Pax. In *Flora of Tropical Africa*; L. Reeve & Co. Ltd.: London, UK, 1913; Volume 6, pp. 538–539.
32. Schlage, C.; Mabula, C.; Mahunnah, R.L.A.; Heinrich, M. Medicinal plants of the Washambaa (Tanzania): Documentation and ethnopharmacological evaluation. *Plant Biol.* **2000**, *2*, 83–92. [CrossRef]
33. Chrispin, F.S.; Innocent, J.E.Z.; Patrick, L.P.M.; Matti, N. Use of medicinal plants in the eastern arc mountains with special reference to the hehe ethnic group in the Udzungwa mountains, Tanzania. *J. East Afr. Nat. Hist.* **2008**, *97*, 225–254.
34. Wang, L.; Yang, J.; Kong, L.M.; Deng, J.; Xiong, Z.J.; Huang, J.P.; Luo, J.P.; Yan, Y.J.; Hu, Y.K.; Li, X.N.; et al. Natural and semisynthetic tigliane diterpenoids with new carbon skeletons from *Euphorbia dracunculoides* as a Wnt signaling pathway inhibitor. *Org. Lett.* **2017**, *19*, 3911–3914. [CrossRef]
35. Aljancic, I.S.; Pesic, M.; Milosavljevic, S.M.; Todorovic, N.M.; Jadranin, M.; Miosavljevic, G.; Povrenovic, D.; Bankovic, J.; Tanic, N.; Markovic, I.D.; et al. Isolation and biological evaluation of jatrophane diterpenoids from *Euphorbia dendroides*. *J. Nat. Prod.* **2011**, *74*, 1613–1620. [CrossRef]
36. Marco, J.A.; Sanz-Cervera, J.F.; Yuste, A.; Jakupovic, J. Isoterracinolides A and B, novel bishomoditerpene lactones from *Euphorbia terracina*. *J. Nat. Prod.* **1999**, *62*, 110–113. [CrossRef]
37. Huang, Y.; Aisa, H.A. Three new diterpenoids from *Euphorbia sororia* L. *Helv. Chim. Acta* **2010**, *93*, 1156–1161. [CrossRef]
38. Hu, R.; Gao, J.; Rozimamat, R.; Aisa, H.A. Jatrophane diterpenoids from *Euphorbia sororia* as potent modulators against P-glycoprotein-based multidrug resistance. *Eur. J. Med. Chem.* **2018**, *146*, 157–170. [CrossRef] [PubMed]
39. Corea, G.; Fattorusso, E.; Lanzotti, V.; Taglialatela-Scafati, O.; Appendino, G.; Ballero, M.; Sirnon, P.N.L.; Dumontet, C.; Di Pietro, A. Modified jatrophane diterpenes as modulators of multidrug resistance from *Euphorbia dendroides* L. *Bioorgan. Med. Chem.* **2003**, *11*, 5221–5227. [CrossRef] [PubMed]

40. Lu, D.L.; Liu, Y.Q.; Aisa, H.A. Jatrophane diterpenoid esters from *Euphorbia sororia* serving as multidrug resistance reversal agents. *Fitoterapia* **2014**, *92*, 244–251. [CrossRef] [PubMed]
41. Marco, J.A.; Sanz-Cervera, J.F.; Yuste, A.; Jakupovic, J.; Jeske, F. Jatrophane derivatives and a rearranged jatrophane from *Euphorbia terracina*. *Phytochemistry* **1998**, *47*, 1621–1630. [CrossRef]
42. Zhang, D.D.; Zhou, B.; Yu, J.H.; Xu, C.H.; Ding, J.; Zhang, H.; Yue, J.M. Cytotoxic tigliane-type diterpenoids from *Croton tiglium*. *Tetrahedron* **2015**, *71*, 9638–9644. [CrossRef]
43. Marco, J.A.; Sanz-Cervera, J.F.; Checa, J.; Palomares, E.; Fraga, B.M. Jatrophane and tigliane diterpenes from the latex of *Euphorbia obtusifolia*. *Phytochemistry* **1999**, *52*, 479–485. [CrossRef]
44. Ara, I.; Siddiqui, B.S.; Faizi, S.; Siddiqui, S. Tricyclic diterpenoids from root bark of *Azadirachta Indica*. *Phytochemistry* **1990**, *29*, 911–914. [CrossRef]
45. Corral, J.M.M.D.; Gordaliza, M.; Salinero, M.A.; Feliciano, A.S. ^{13}C NMR data for abieta-8,11,13-triene diterpenoids. *Magn. Reson. Chem.* **1994**, *32*, 774–781. [CrossRef]
46. Seca, A.M.L.; Silva, A.M.S.; Bazzocchi, I.L.; Jimenez, I.A. Diterpene constituents of leaves from *Juniperus brevifolia*. *Phytochemistry* **2008**, *69*, 498–505. [CrossRef]
47. Lal, A.R.; Cambie, R.C.; Rutledge, P.S.; Woodgate, P.D. Ent-pimarane and ent-abietane diterpenes from *Euphorbia fidjiana*. *Phytochemistry* **1990**, *29*, 2239–2246. [CrossRef]
48. Talapatra, S.K.; Das, G.; Talapatra, B. Stereostructures and molecular conformations of six diterpene lactones from *Gelonium multiflorum*. *Phytochemistry* **1989**, *28*, 1181–1185. [CrossRef]
49. Wang, H.; Zhang, X.F.; Cai, X.H.; Ma, Y.B.; Luo, X.D. Three new diterpenoids from *Euphorbia wallichii*. *Chin. J. Chem.* **2004**, *22*, 199–202. [CrossRef]
50. Choudhary, M.I.; Gondal, H.Y.; Abbaskhan, A.; Jahan, I.A.; Parvez, M.; Nahar, N.; Rahman, A. Revisiting diterpene lactones of *Suregada multiflora*. *Tetrahedron* **2004**, *60*, 7933–7941. [CrossRef]
51. Song, Q.Q.; Rao, Y.; Tang, G.H.; Sun, Z.H.; Zhang, J.S.; Huang, Z.S.; Yin, S. Tigliane diterpenoids as a new type of antiadipogenic agents inhibit GR alpha-Dexras1 axis in adipocytes. *J. Med. Chem.* **2019**, *62*, 2060–2075. [CrossRef]
52. Yin, S.; Huang, Z.; Rao, Y.; Tang, G.; Song, Q. Tigliane-type diterpenoid compounds and preparation method and application thereof. China Patent CN108689851A, 28 May 2018.
53. Guo, K.; Liu, Y.C.; Liu, Y.; Luo, S.H.; Li, W.Y.; Li, X.N.; Li, S.H. Diversified abietane family diterpenoids from the leaves of *Leucosceptrurn canum* and their cytotoxic activity. *Phytochemistry* **2019**, *157*, 43–52. [CrossRef]
54. Borghi, D.; Baumer, L.; Ballabio, M.; Arlandini, E.; Perellino, N.C.; Minghetti, A.; Vincieri, F.F. Structure elucidation of helioscopinolides D and E from *Euphorbia calyptrata* cell cultures. *J. Nat. Prod.* **1991**, *54*, 1503–1508. [CrossRef]
55. Tori, M.; Arbiyanti, H.; Taira, Z.; Asakawa, Y. Terpenoids of the liverwort *Frullanoides densifolia* and *Trocholejeunea sandvicensis*. *Phytochemistry* **1993**, *32*, 335–348. [CrossRef]
56. Arisawa, M.; Handa, S.S.; McPherson, D.D.; Lankin, D.C.; Cordell, G.A.; Fong, H.H.S.; Farnsworth, N.R. Plant anticancer agents XXIX. Cleomiscosin A from *Simaba multiflora*, *Soulamea soulameoides*, and *Matayba arborescens*. *J. Nat. Prod.* **1984**, *47*, 300–307. [CrossRef]
57. Min, Y.D.; Choi, S.U.; Lee, K.R. Aporphine alkaloids and their reversal activity of multidrug resistance (MDR) from the stems and rhizomes of *Sinomenium acutum*. *Arch. Pharm. Res.* **2006**, *29*, 627–632. [CrossRef] [PubMed]
58. Valcic, S.; Montenegro, G.; Timmermann, B.N. Lignans from *Chilean propolis*. *J. Nat. Prod.* **1998**, *61*, 771–775. [CrossRef] [PubMed]
59. Bao, K.; Fan, A.X.; Dai, Y.; Zhang, L.; Zhang, W.G.; Cheng, M.S.; Yao, X.S. Selective demethylation and debenzylation of aryl ethers by magnesium iodide under solvent-free conditions and its application to the total synthesis of natural products. *Org. Biomol. Chem.* **2009**, *7*, 5084–5090. [CrossRef]
60. Kim, H.; Ralph, J.; Lu, F.C.; Ralph, S.A.; Boudet, A.M.; MacKay, J.J.; Sederoff, R.R.; Ito, T.; Kawai, S.; Ohashi, H.; et al. NMR analysis of lignins in CAD-deficient plants. Part 1. Incorporation of hydroxycinnamaldehydes and hydroxybenzaldehydes into lignins. *Org. Biomol. Chem.* **2003**, *1*, 268–281. [CrossRef]
61. Yao, C.S.; Lin, M.; Wang, L. Isolation and biomimetic synthesis of anti-inflammatory stilbenolignans from *Gnetum cleistostachyum*. *Chem. Pharm. Bull.* **2006**, *54*, 1053–1057. [CrossRef]
62. Duarte, N.; Ferreira, M.J.U. Lagaspholones A and B: Two new jatropholane-type diterpenes from *Euphorbia lagascae*. *Org. Lett.* **2007**, *9*, 489–492. [CrossRef] [PubMed]
63. De la Torre-Tarazona, H.E.; Jimenez, R.; Bueno, P.; Camarero, S.; Roman, L.; Fernandez-Garcia, J.L.; Beltran, M.; Nothias, L.F.; Cachet, X.; Paolini, J.; et al. 4-Deoxyphorbol inhibits HIV-1 infection in synergism with antiretroviral drugs and reactivates viral reservoirs through PKC/MEK activation synergizing with vorinostat. *Biochem. Pharmacol.* **2020**, *177*, 113937. [CrossRef]
64. Hammadi, R.; Kúsz, N.; Dávid, C.Z.; Behány, Z.; Papp, L.; Kemény, L.; Hohmann, J.; Lakatos, L.; Vasas, A. Ingol and ingenol-type diterpenes from *Euphorbia trigona* Miller with keratinocyte inhibitory activity. *Plants* **2021**, *10*, 1206. [CrossRef]
65. Jiang, G.; Maverakis, E.; Cheng, M.Y.; Elsheikh, M.M.; Deleage, C.; Mendez-Lagares, G.; Shimoda, M.; Yukl, S.A.; Hartigan-O'Connor, D.J.; Thompson, G.R.; et al. Disruption of latent HIV *in vivo* during the clearance of actinic keratosis by ingenol mebutate. *JCI Insight* **2019**, *4*, e126027. [CrossRef]